

AD-A042 083

BOEING VERTOL CO PHILADELPHIA PA
INVESTIGATION OF AEROELASTICALLY ADAPTIVE ROTORS.(U)

F/G 1/3

UNCLASSIFIED

MAY 76 G S DOMAN, F J TARZANIN, J SHAW

DAAJ02-75-C-0040

D238-10003-1

USAAMRDL-TR-77-3

NL

| OF |

ADAO42083



AD A 042083

USAAMRDL-TR -77-3

12



2

INVESTIGATION OF AEROELASTICALLY ADAPTIVE ROTORS

Boeing Vertol Company
P. O. Box 16858
Philadelphia, Pa. 19142

May 1977

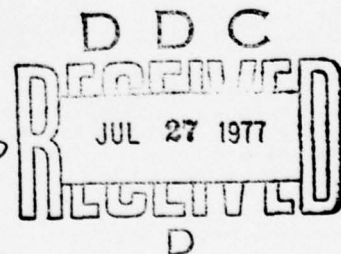
Final Report for Period June 1975 to October 1976

Approved for public release;
distribution unlimited.

Prepared for

EUSTIS DIRECTORATE

U. S. ARMY AIR MOBILITY RESEARCH AND DEVELOPMENT LABORATORY
Fort Eustis, Va. 23604



EUSTIS DIRECTORATE POSITION STATEMENT

This report has been reviewed by the Eustis Directorate, U.S. Army Air Mobility Research and Development Laboratory and is considered to be technically sound. This program was initiated to investigate the improvement of helicopter rotor productivity through changing the aeroelastic behavior of rotor blades and to quantify the productivity gains that would derive from the application of favorable aeroelastic design features with emphasis on improving payload, vibratory load attenuation, noise, and hover.

This program was conducted under the technical management of Mr. D. J. Merkley, Aeromechanics Technical Area, Technology Applications Division of this Directorate.

DISCLAIMERS

The findings in this report are not to be construed as an official Department of the Army position unless so designated by other authorized documents.

When Government drawings, specifications, or other data are used for any purpose other than in connection with a definitely related Government procurement operation, the United States Government thereby incurs no responsibility nor any obligation whatsoever; and the fact that the Government may have formulated, furnished, or in any way supplied the said drawings, specifications, or other data is not to be regarded by implication or otherwise as in any manner licensing the holder or any other person or corporation, or conveying any rights or permission, to manufacture, use, or sell any patented invention that may in any way be related thereto.

Trade names cited in this report do not constitute an official endorsement or approval of the use of such commercial hardware or software.

DISPOSITION INSTRUCTIONS

Destroy this report when no longer needed. Do not return it to the originator.

Unclassified

SECURITY CLASSIFICATION OF THIS PAGE (When Data Entered)

REPORT DOCUMENTATION PAGE		READ INSTRUCTIONS BEFORE COMPLETING FORM	
1. REPORT NUMBER USAAMRDI TR-77-3	2. GOVT ACCESSION NO.	3. RECIPIENT'S CATALOG NUMBER	
4. TITLE (and Subtitle) INVESTIGATION OF AEROELASTICALLY ADAPTIVE ROTORS.	5. TYPE OF REPORT - PERIOD COVERED Final Report. 20 Jun 75 - 20 Oct 76	6. PERFORMING ORG. REPORT NUMBER D238-10003-1	
7. AUTHOR(S) Glidden S. Doman, Frank J. Tarzanin, Jr. John Shaw, Jr.	8. CONTRACT OR GRANT NUMBER(s) DAAJ02-75-C-0040	9. PERFORMING ORGANIZATION NAME AND ADDRESS Boeing Vertol Company P.O. Box 16858 Philadelphia, PA 19142	
10. CONTROLLING OFFICE NAME AND ADDRESS Eustis Directorate U.S. Army Air Mobility Research & Development Lab, Fort Eustis, VA 23604	11. PROGRAM ELEMENT, PROJECT, TASK AREA & WORK UNIT NUMBERS 62209 IF262209AH76 00 086 EK	12. REPORT DATE May 1976	
13. MONITORING AGENCY NAME & ADDRESS (if different from Controlling Office) 1269p.	14. SECURITY CLASS. (of this report) Unclassified	15. SECURITY CLASS. (of this report) Unclassified	
16. DISTRIBUTION STATEMENT (of this Report) Approved for public release. Distribution unlimited.			
17. DISTRIBUTION STATEMENT (of the abstract entered in Block 20, if different from Report)			
18. SUPPLEMENTARY NOTES			
19. KEY WORDS (Continue on reverse side if necessary and identify by block number)			
Helicopter	Torsional Stiffness	Rotor Limits	
Rotor	Aerodynamic Pitching	Fatigue Loads	
Aeroelasticity	Moment	Aerodynamic	
Dynamic Blade Twist	Blade Sweep	Efficiency	
20. ABSTRACT (Continue on reverse side if necessary and identify by block number) Basic principles of aeroelastically adaptive rotor systems have been investigated by wind tunnel test and theory. These are helicopter rotor systems in which dynamic blade twist is enhanced and managed to extend rotor operating limits to higher lifts and advance ratios. In wind tunnel testing, dynamic twist was induced in blades of relatively low torsional stiffness using two design features shown by theoretical analysis to have significant			

DD FORM 1 JAN 73 1473

EDITION OF 1 NOV 65 IS OBSOLETE

Unclassified

SECURITY CLASSIFICATION OF THIS PAGE (When Data Entered)

403 682

Unclassified

SECURITY CLASSIFICATION OF THIS PAGE(When Data Entered)

20. Abstract (Continued)

potential: airfoil pitching moment and blade planform sweep with the sweep apex near midspan. Effects on trim, flying qualities, fatigue loads, and aerodynamic efficiency were measured. Theory was used to explore specific design applications and to assess potential for productivity improvement.

ACCESSION for	
NTIS	White Section <input checked="" type="checkbox"/>
DDC	Buff Section <input type="checkbox"/>
UNANNOUNCED	<input type="checkbox"/>
JUSTIFICATION	
BY	
DISTRIBUTION/AVAILABILITY CODES	
Dist.	AVAIL. and/or SPECIAL
A	

DDC
RECEIVED
JUL 27 1977
D

Unclassified

SECURITY CLASSIFICATION OF THIS PAGE(When Data Entered)

SUMMARY

Two 10-foot-diameter model rotors were tested in the Boeing Vertol 20-foot V/STOL wind tunnel. These models were variants of a four-bladed, soft-inplane, hingeless main-rotor model, which was tested in support of the UTTAS YUH-61A program. One rotor had all the exterior blade contours of the YUH-61A, while the other had a 10-degree sweepback of the planform with the sweep apex at 65-percent span. Both had blade torsional stiffness reduced by about 80 percent and had provision for introduction of aerodynamic pitching moment, C_{M_0} , by trailing edge deflection.

The purpose of the testing and of the related analytical work was exploration of the basic principles of aeroelastically adaptive rotor systems. Overall goal of this research is the enhancement and management of dynamic blade twist to increase helicopter productivity by extending rotor operating limits.

Rotor operating limits, whatever their source -- stall and reverse flow which limit capability directly, or the associated fatigue loads, vibration, noise, and power requirements which normally restrict operation by imposing increasing costs -- essentially result from unfavorable airload distributions, both spanwise and azimuthal. Dynamic blade twist is a powerful means of improving these distributions. Thus, projected aeroelastically adaptive rotors are expected to have favorable dynamic twist which adapts to the operating condition.

Candidate design features are also being examined for their value in enabling the rotor to adapt at high advance ratio to the following desirable design changes:

- Increased static twist, which improves hover performance but normally increases fatigue loads in forward flight.
- Two-per-rev root pitch, which is expected to extend propulsive force limits but also increase blade fatigue loads.

In these wind tunnel tests, dynamic twist has been induced in blades of reduced torsional stiffness by adjusting C_{M_0} and by sweepback of the outer 35 percent of the blade planform. Two-per-rev root pitch control of the torsionally softened blades has also been examined.

Because of mechanical limitations in the control system, the wind tunnel models could not be flown to their limits of

propulsive capability. Therefore, the effects of the induced dynamic twist upon propulsive limits could not be directly observed.

Dynamic twist responses and related effects in the model with blades of straight planform were predicted by the Boeing Vertol rotor dynamic analytical program C60. The degree of success which was attained substantiated the program as an engineering tool for that use.

C60 substantiation for the swept-planform blades has been impeded by the presence of a flap bending/torsion instability seen in the swept-bladed model. Thus, program modifications which incorporate sweep effects in C60 are not yet known to be successful. Efforts to stabilize the swept physical model and to validate the analysis are continuing.

Test results show that flap bending at high advance ratios can be reduced significantly by proper choice of C_{M_0} , so that static twist can be increased to improve hover performance. Significant amounts of two-per-rev dynamic twist have been induced in varying azimuthal phases, pointing to combinations of design features which should unload the retreating blade at high advance ratio, with potential gains in rotor limits of all types. Finally, the operation of planform sweep as a physical feedback-type bending load attenuator has been demonstrated, showing the value of this feature in attaining rotor adaptability.

The dynamic twists which attenuate outboard flap bending were found to have generally favorable effects upon flying qualities, principally an increase of speed stability. No adverse effects upon aerodynamic efficiency were found.

In theory, the twists which attenuate flap bending should reduce the advance ratios at which rotor propulsive limits are reached. This adverse effect must be quantified in future testing so that its significance to helicopter productivity can be evaluated. Means for offsetting this effect and increasing the propulsive limit also remain to be investigated.

Preliminary performance investigation has quantified the gains which can be realized by an aeroelastically adaptive design that permits operation of the Boelkow/Boeing BO-105 helicopter at 600 fps tip speed (compared to the present 716 fps), and 18-degree linear steady twist (compared to the present 8 degrees). Without any reduction of the present 145 knot top speed, the resulting gains would include 13 percent reduction of hovering power required, 156 percent increase of vertical rate of climb, and a 4-decibel reduction of main rotor noise. Aural detection distance against a moderate ambient noise background would be decreased 33 percent.

TABLE OF CONTENTS

	<u>Page</u>
SUMMARY	3
LIST OF ILLUSTRATIONS.....	7
LIST OF TABLES	8
INTRODUCTION	9
DISCUSSION OF AEROELASTIC ADAPTIVITY	10
An Aeroelastic Approach to Productivity Improvement ...	10
The Fundamentals of Airload Redistribution	12
Selection of Dynamic Twist Sources	14
WIND TUNNEL TESTING	16
Test Objectives	16
Model Description	16
Test Procedure	26
OBSERVED EXPERIMENTAL RESULTS	29
Harmonic Content of Data	29
Effects of Pitching Moment Coefficient, C_{M_0}	29
Effects of Outboard Planform Sweep	38
Effects of Second-Harmonic Root Pitch	48
PRESENT AND FUTURE ROLE OF ANALYTICS	50
Prediction of C_{M_0} Effects on Straight Blades	50
Torsion Calculation is Most Essential	53
Prediction of the Effects of Planform Sweep	53
General Adequacy of Analytical Tools	57
ANALYTICAL STUDY OF DESIGN APPLICATIONS	58
Improvement of Hover Performance	58
Reduction of Flap Bending at High Speed	61
Combined Gains	61
APPLICATION TO A DEMONSTRATION ROTOR	63
Selection of a Baseline Helicopter	63
Adjustment of Twist and Tip Speed	64
Propulsive Capability Effects	65
Projected Gains	65

	<u>Page</u>
CONCLUSIONS	67
Straight Planform Blades	67
Swept Planform Blades	67
Combination of Sweep and C_{M_0} Effects	68
Retention of Propulsive Capability	68
Compatibility of Second-Harmonic Root Pitch Control	69
LIST OF SYMBOLS	70

LIST OF ILLUSTRATIONS

<u>Figure</u>		<u>Page</u>
1	Model Rotor with Outboard Planform Sweep - Installed in Wind Tunnel	17
2	Comparison of Blade Properties	18
3	Wind Tunnel Test Envelope Imposed by Model Control System Limitations	27
4	C_{M_0} Effect on Cyclic Trim : Straight, Soft Blade (Design 6)	31
5	C_w Effect on Flap Bending at 0.63R : Straight, ft Blade (Design 6)	32
6	C_{M_0} Effect on Aerodynamic Efficiency: Straight, Soft Blade (Design 6)	33
7	C_{M_0} Effect on Cyclic Trim : Swept, Soft Blade (Design 5)	35
8	C_{M_0} Effect on Flap Bending at 0.67R: Swept, Soft Blade (Design 5)	36
9	C_{M_0} Effect on Aerodynamic Efficiency : Swept, Soft Blade (Design 5)	37
10	Aeroelastic Stability Limits of Swept, Soft Blades (Design 5)	39
11	Modal Frequencies Observed with On-line Spectral Analyzer: Swept, Soft Blades (Design 5)	40
12	Outboard Sweep Effect on Cyclic Trim: Zero Tab . .	41
13	Outboard Sweep Effect on Flap Bending at 0.63R: Zero Tab	42
14	Outboard Sweep Effect on Aerodynamic Efficiency: Zero Tab	43

<u>Figure</u>	<u>Page</u>
15 Outboard Sweep Effect on Cyclic Trim : $\Delta C_{M_O} = 0.033$	44
16 Outboard Sweep Effect on Flap Bending at 0.067R : $\Delta C_{M_O} = 0.033$	45
17 Outboard Sweep Effect on Aerodynamic Efficiency : $\Delta C_{M_O} = 0.033$	46
18 Alternating Flap Bending: C-60 Prediction Versus Wind Tunnel Data for Straight, Soft Blade (Design 6)	51
19 Flap Bending Waveform at 0.48R: C-60 Prediction Versus Wind Tunnel Data for Straight, Soft Blade (Design 6)	52
20 Modal Frequencies of Swept, Soft Blade (Design 5): Y69 and Y71 Predictions	56
21 Hover Power Required Versus Static Twist and C_{M_O} : C-60 Prediction for Straight, Soft Blade	59
22 Alternating Midspan Flap Bending Versus Static Twist and C_{M_O} : C-60 Prediction for Straight, Soft Blade	60

LIST OF TABLES

<u>Table</u>		
1	Standard BO-105 Vehicle and Rotor System Characteristics	63
2	Gains Achievable in a BO-105 Helicopter Using Aeroelastically Adaptive Design Features	65

INTRODUCTION

Design for helicopter flight at substantially increased advance ratios is the central goal of a current research program which seeks benefits from passively induced vibratory twist of the rotor blade. This research is intended to increase vehicle productivity without increasing complexity; therefore, it is limited to wingless flight where all propulsion is obtained from the rotor.

The only active physical feature being investigated, and not present in contemporary designs, is second harmonic pitch control of the blade root. If it is concluded that this is a cost-effective means of increasing the advance ratio which can be flown, attention must be given to side effects upon rotor behavior. These side effects will then be added to the conditions for which aeroelastic adaptivity of the blade is being sought.

This report introduces the technical approach that is being taken in seeking favorable aeroelastic adaptivity of the rotor blade to the high-speed operating environment. It also presents the findings which have so far come from analytical investigations and wind tunnel tests.

DISCUSSION OF AEROELASTIC ADAPTIVITY

AN AEROELASTIC APPROACH TO PRODUCTIVITY IMPROVEMENT

Productivity of contemporary helicopters is limited by speed, lift, and altitude restrictions which involve the aeroelastic behavior of the rotor -- limits imposed by vibration, noise, fatigue loads, and increased power requirements. Research aimed at productivity improvement must therefore address the question:

*CAN THE AEROELASTIC BEHAVIOR OF THE BLADE BE CHANGED
AND CONTROLLED IN A MANNER WHICH WILL OPEN THE DESIGN
OPERATING LIMITS OF THE ROTOR?*

Examination of the several ways in which rotor limits are encountered shows that they stem from two problems of load distribution over the area of the rotor disk:

- Unfavorable spanwise distributions.
- Unfavorable azimuthal distributions.

Both lead to vibratory bending loads and increased power requirements. The unfavorable azimuthal distributions also lead to thrust limits and propulsive force limits at higher advance ratios.

Because the blade has finite torsional stiffness, it is clear that dynamic twist always enters the picture to alter the aerodynamic load distributions -- perhaps favorably, perhaps unfavorably. It has been postulated in this program that because increased dynamic twist can have a major effect on the airload distributions, and because powerful design features are available to control the twist, the above question can be answered affirmatively.

There is no initial concern in this research with the usual design variables such as solidity, disk loading, tip speed, and number of blades per rotor. Instead, interest is centered on a new set of variables which influence aeroelastic behavior. The conventional parameters can later be varied over and above the aeroelastic parameters to synthesize and evaluate helicopter designs with productivity gains directed at specific missions.

Design Compromises Currently Forced by Character of Blade Loading

Rotor lifting efficiency in hover can be improved by increasing the static twist of the blade. However, an increase of static twist causes a more rapid growth of blade-bending vibratory loads as the speed of forward flight

increases. And when forward speed and rotor loading combine to cause stall of the outboard retreating blade while it is developing substantial lift, the ill effects of vibratory blade loading are compounded by stall-associated vibratory loads.

At present, designers are forced to compromise hover performance and to yield to increased rotor noise because of the maldistribution of airloads during high-speed flight. Excessive tip speed and insufficient static twist are employed. Relief from these compromises is sought by improving the dynamics of the rotor at high advance ratios.

This effort is not so concerned with response dynamics in the usual sense; instead, it seeks to redistribute the airloads that force the blade -- to change them in a manner which will open the limits on performance and productivity.

The Role of Data from Past Test Programs

The azimuthal distributions, spanwise distributions, and harmonic content of the airloading on a rotor blade result from a highly complex interaction of unsteady conditions which no one fully understands. No present-day computer model can account rigorously for the interaction of blade elastic deformation and downwash. Simplifying assumptions and accumulated cause-and-effect observations converted to design criteria form much of the current technology.

Yet it has seemed likely that the introduction of corrective aeroelastic behavior could favorably alter blade airloads and that the causes of such loads need not be understood in full as a prerequisite to their attenuation. A study of the detailed character of the airloads on actual helicopter blades was thus suggested, independent of any limits upon understanding their causes.

Flight test data from the contractual research programs reported in References 1, 2 and 3 were therefore examined in some detail. Included were airload measurements and strain

1. Beno, Edward A., CH-53A MAIN ROTOR AND STABILIZER VIBRATORY AIRLOADS AND FORCES, Volume II, Sikorsky Aircraft Division, United Technologies Corporation, Stratford, Connecticut, SER 65593; Naval Air Systems Command, Department of the Navy, Washington, D.C., June 1970.
2. Bartsch, E.A., IN-FLIGHT MEASUREMENTS AND CORRELATION WITH THEORY OF BLADE AIRLOADS AND RESPONSES ON THE XH-51A COMPOUND HELICOPTER ROTOR, Volume I, Measurement and Data Reduction of Airloads and Structural Loads, Lockheed-California Company, Burbank, California; USAAVLABS Technical Report 68-22A, U.S. Army Air Mobility Research and Development Laboratory, Fort Eustis, Virginia, May 1968, AD67419(3).

gage data obtained in high-speed flight and in the transition to forward flight of the fully articulated CH-53A, the semi-rigid (teetering) UH-1A, and the hingeless XH-51A rotors. The phase angles and spanwise distributions of the principal harmonics of airloads were remarkably similar in these three rotor systems, and the bending-load distributions and phases were predictably related to the hub configurations and to the modal natural frequencies. This flight test data revealed a constancy of character of the principal airloads and suggested blade design features which should cause favorable redistribution of these airloads.

THE FUNDAMENTALS OF AIRLOAD REDISTRIBUTION

The ill effects of high advance ratio divide into those due to growth of vibratory flap bending and those due to retreating blade lift deficiency. Flap bending can be reduced by inducing periodic blade twist. Retreating blade lift deficiency can be offset by providing periodic pitch change effects, either as twist or as root pitch control, of suitable second-harmonic character.

Flap Bending

Attenuation of flap bending has the prime purpose of opening the limits now imposed by structural fatigue and vibration problems. Its achievement will permit the increase of design static twist to values which have previously induced excessive flap bending at high advance ratio. Thus it can open the way to improved hover performance. Improved forward flight aerodynamic efficiency may also accrue from the implicit smoothing of downwash distribution. Elimination of the down loads now typically seen on the advancing blade tip should appear and be a significant source of performance improvement. Reduction of downloads now carried in the reverse flow region is another performance benefit which may accrue from improvement of the airload distribution.

First-harmonic twist of a sine ψ phase (nose up at the advancing side of the disc) is the obvious first step toward improvement of the bending loads and load maldistribution seen in the advancing/retreating profile of the rotor. If sine ψ twist of a suitable spanwise distribution could clean up the first-harmonic bending there would remain a second, a third, and higher harmonics of bending. The second and third harmonics are clearly worthy of attention and each would

3. Burpo, F.B., and Lynn, R.R., MEASUREMENT OF DYNAMIC AIR LOADS ON A FULL-SCALE SEMIRIGID ROTOR, Bell Helicopter Company, Fort Worth, Texas; TREC Technical Report 62-42, U.S. Army Air Mobility Research and Development Laboratory, Fort Eustis, Virginia, December 1962.

require a superimposed twist of suitable spanwise profile, phase, and harmonic order.

While it is not expected that all these conditions can be satisfied by passive design features in the blade, it is postulated that large gains can be made by qualitative attack upon the major and dominant problems. Test results are confirming that the desired gains can indeed be achieved.

Twists of an approximately correct spanwise profile and of required harmonic order can be induced suitably and separately. Their amplitudes and phases can be selectively controlled by choice of passive design features of the blade. The quantities of twist which are structurally feasible are sufficient to attain major attenuation of flap bending. Trade-offs of these gains versus blade cost and ruggedness factors will get increasing attention as the project progresses.

Retreating Blade Lift Deficiency

Because the conventional means of controlling and trimming the rotor requires lift moment from the retreating blade, the increase of advance ratio leads to outboard stall under load and to associated loss of propulsive capability. The terminology "stall under load" indicates stall which results from increasing the airfoil angle of attack at significant relative velocities, which on the retreating blade would occur outboard of the reverse flow region.

If collective and first-harmonic cyclic pitch are the only control effects provided, a propulsive limit is reached when adequate lift moment can no longer be obtained from the retreating blade. For contemporary rotor systems flown without a lift-sharing wing, an absolute limit of propulsive capability is reached in level flight at an advance ratio of about 0.7. This occurs because further lift moment from the retreating blade becomes unavailable.

A solution lies in reducing the lift moment demanded in the vicinity of $\psi = 270$ degrees. This may be done by increasing $\cos 2\psi$ lift (increasing the lift over the nose and tail). It requires a $\cos 2\psi$ pitch effect which may be in the form of $\cos 2\psi$ twist or of second harmonic pitch effects at the blade root. However accomplished, the increased $\cos 2\psi$ lift will unload the retreating blade for a given state of cyclic trim, thus allowing an increase of collective pitch to be applied either for speed increase or maneuvering thrust increase. Retreating blade stall will then occur under low load at low relative velocities, rather than from excessive load and angle of attack as at present. This approach holds the prospect of opening the flyable limits to significantly higher advance ratios.

In addition to loss of propulsive capability, outboard stall under load results in increased control loads and power requirements. By achieving increased $\cos 2\psi$ lift and eliminating the retreating blade stall under load, the stall-induced power loss and control load increases will be eliminated. If, however, further demands are placed on the rotor by high maneuvering rotor thrust as an example, the resulting retreating blade stall under load need not result in large stall flutter loads. This conclusion is based on the observation that the low blade torsional stiffness of the aeroelastically adaptive rotor will tend to reduce stall flutter, as was shown in Reference 4.

SELECTION OF DYNAMIC TWIST SOURCES

Because dynamic twist of the rotor blade can have major effects upon flying qualities, attention must be given to those and other side effects when the blade design is altered to improve structural conditions and speed capability. This is facilitated by the fact that the sources of dynamic twist, which can be altered at will, divide neatly into three types having different relationships to the operating regime.

Camber Effects

Twists induced by airfoil camber are essentially dependent upon rpm and forward speed and independent of thrust. They influence speed stability of the vehicle but they have little effect upon dynamic flight stability. These twists tend to be of large first harmonic ($\sin \psi$) content, of smaller second harmonic content, and negligible at higher orders.

Chordwise Unbalance Effects

Twists induced when elemental chordwise center-of-gravity loci are moved away from the aerodynamic centers are essentially dependent upon forward speed and rotor thrust. They have little effect upon speed stability but have large effects upon dynamic flight stability. These twists tend to be of large second-harmonic and small first-harmonic content in steady trimmed flight. In maneuvers or gusts a transient first-harmonic content appears and influences dynamic stability. Unfortunately, this source of second-harmonic twist cannot be selected to induce the desired $\cos 2\psi$ lift augmentation. The reason is that elemental chordwise center of gravity would have to be moved aft with strong adverse effects upon dynamic stability.

-
4. Tarzanin, F. J. and Mirick, P. H., CONTROL LOAD ENVELOPE SHAPING BY LIVE TWIST, Journal of Aircraft, August 1974.

Outboard Planform Sweep

Twists induced when the outboard blade planform is swept are essentially dependent upon outboard flap bending, whatever its causes. These twists are forced by the bending moments and therefore result in only partial attenuation of the bending. Active at all essential harmonics, the effectiveness of these twists is highly dependent upon lowering the torsional stiffness of the blade. Practical, attainable low stiffnesses do result in useful first and second harmonic bending attenuation. Results at higher harmonics depend upon the torsional natural frequency which, if not properly chosen, can turn the attenuating mechanism into a high-gain loop, or can create instabilities.

WIND TUNNEL TESTING

TEST OBJECTIVES

An early objective of this research program was to determine, experimentally, whether substantial improvements to bending loads and aerodynamic performance could be obtained. The effects of varying C_{M_0} , and of introducing outboard planform sweep were selected for wind tunnel investigation because theory suggested that these changes would be powerful, and perhaps essential. Variation of chordwise mass distribution was deferred because of anticipated adverse side effects.

A preliminary investigation of the effects of second-harmonic control of blade root pitch upon rotor trim, bending loads, and aerodynamic performance was also included in the wind tunnel tests. The objective was to evaluate the side effects of this method of increasing the flyable advance ratio and to determine what additional requirements of aeroelastic adaptivity might be involved.

MODEL DESCRIPTION

Two aeroelastically adaptive rotors were tested in the Boeing Vertol V/STOL wind tunnel, one with a 10-degree sweepback of the planform at 65-percent span (Design 5), and one without the planform sweepback (Design 6). Figure 1 shows the Design 5 swept rotor installed in the tunnel. These models were variants of a 10-foot-diameter, four-bladed, soft-inplane, hingeless main-rotor model that was built and tested in support of the UTTAS YUH-61A program. The Mach-scaled UTTAS model served as a baseline design for comparison with the aeroelastically adaptive rotors. The aeroelastically adaptive blades were built in the UTTAS molds, so that except for the sweep in one set and except for trailing-edge reflex changes made during the test program, external contours were identical to the UTTAS baseline blades. In particular, chord was 4.79 inches, twist was 12 degrees, and the airfoil was the VR-7 inboard of 0.75R, faired linearly to the VR-9 at the tip.

Both sets of aeroelastically adaptive blades were of fiberglass composite construction similar to the UTTAS model, except for internal changes which were designed to reduce their overall torsional stiffness to about 20 percent of that in the baseline blade, and to eliminate the concentrated tip weight and tuning weight of the baseline blade while maintaining the same blade weight and chordwise balance. The internal changes made for stiffness reduction also moved the shear center significantly forward. Physical properties of the three rotor designs are compared in Figure 2.

In the subject research we desired to see effects of and upon the spanwise distribution of airloads. These effects were



Figure 1. Model Rotor with Outboard Planform Sweep -
Installed in Wind Tunnel.

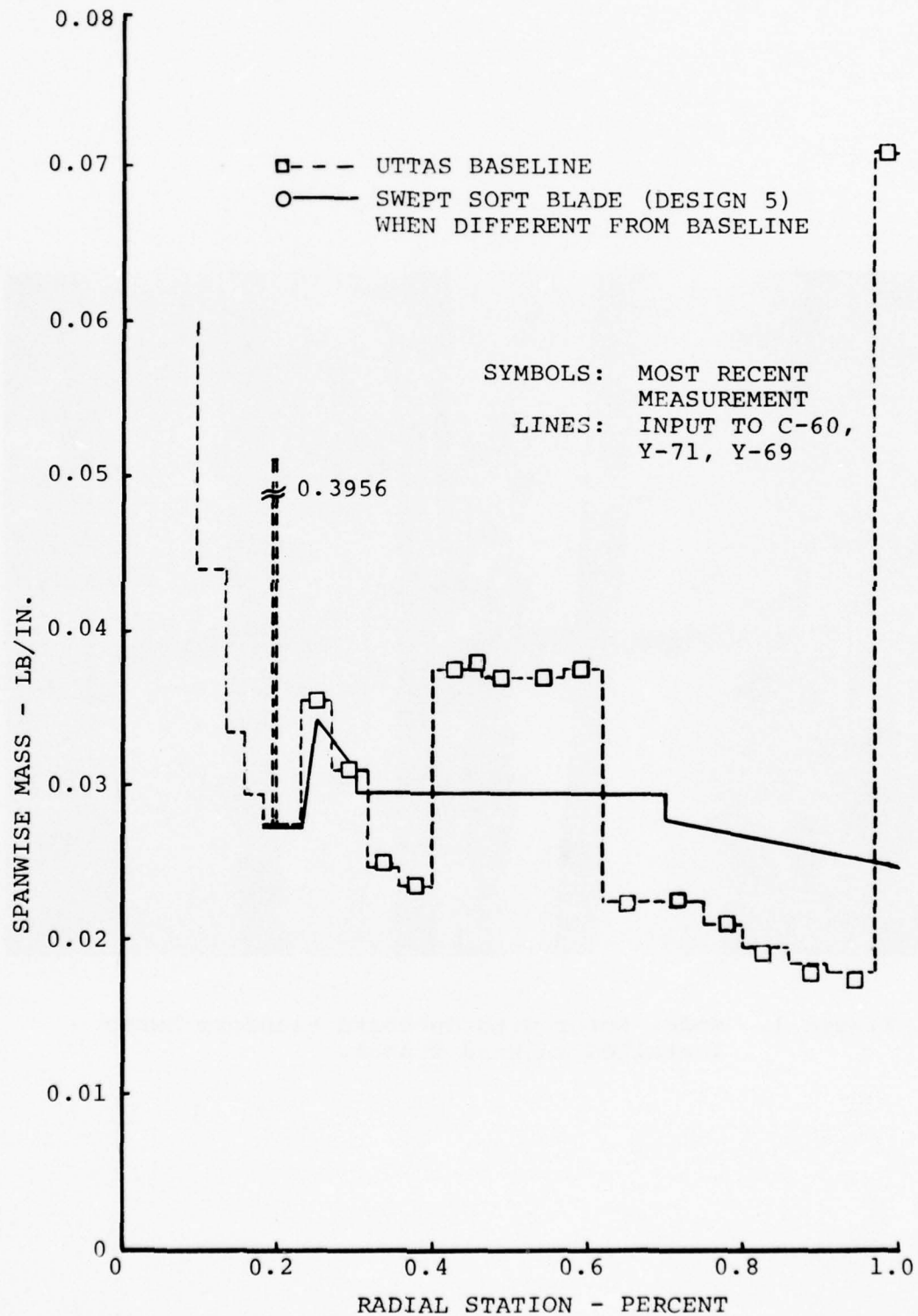


Figure 2. Comparison of Blade Properties (Sheet 1 of 8).

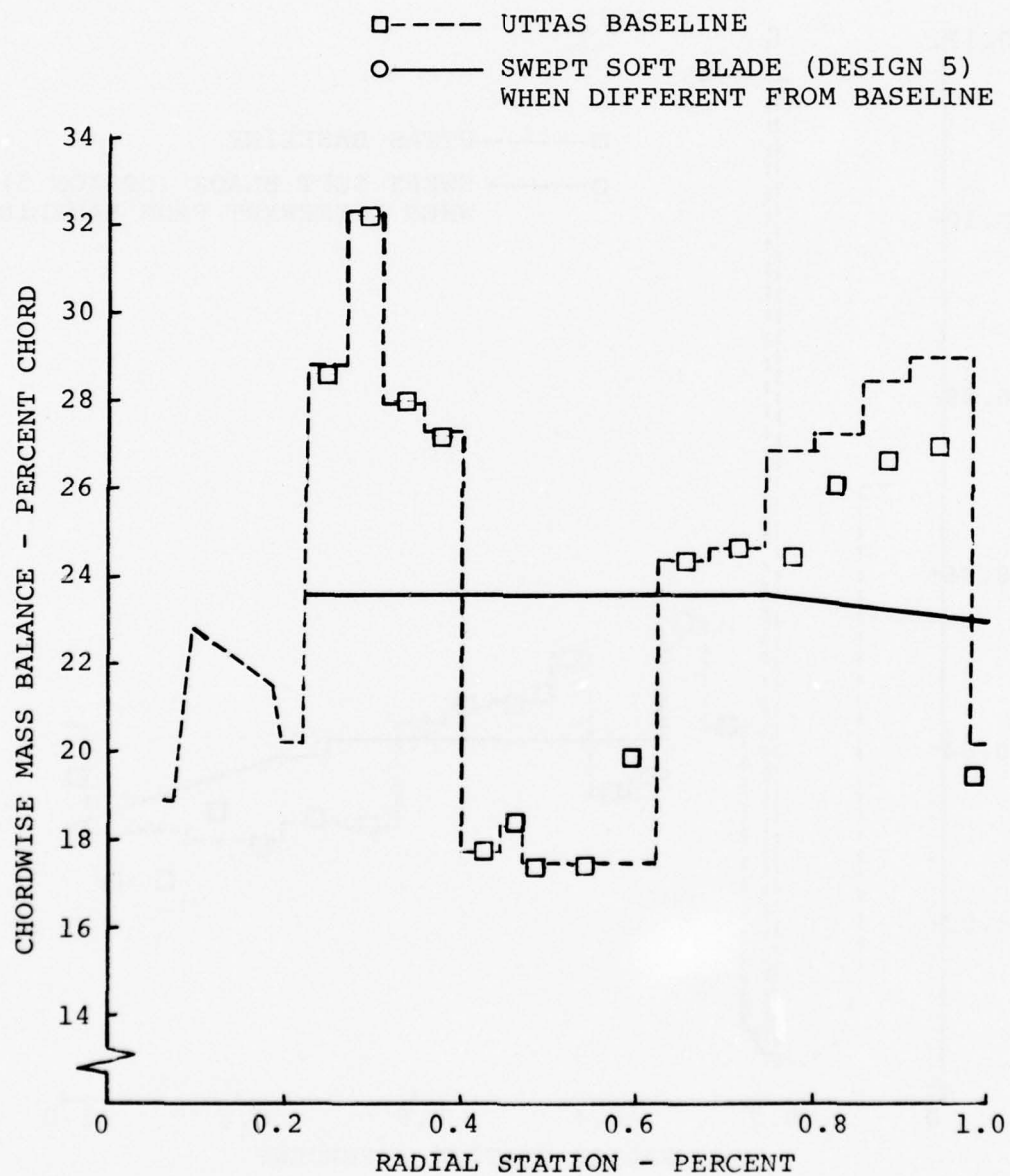


Figure 2. Comparison of Blade Properties (Sheet 2 of 8).

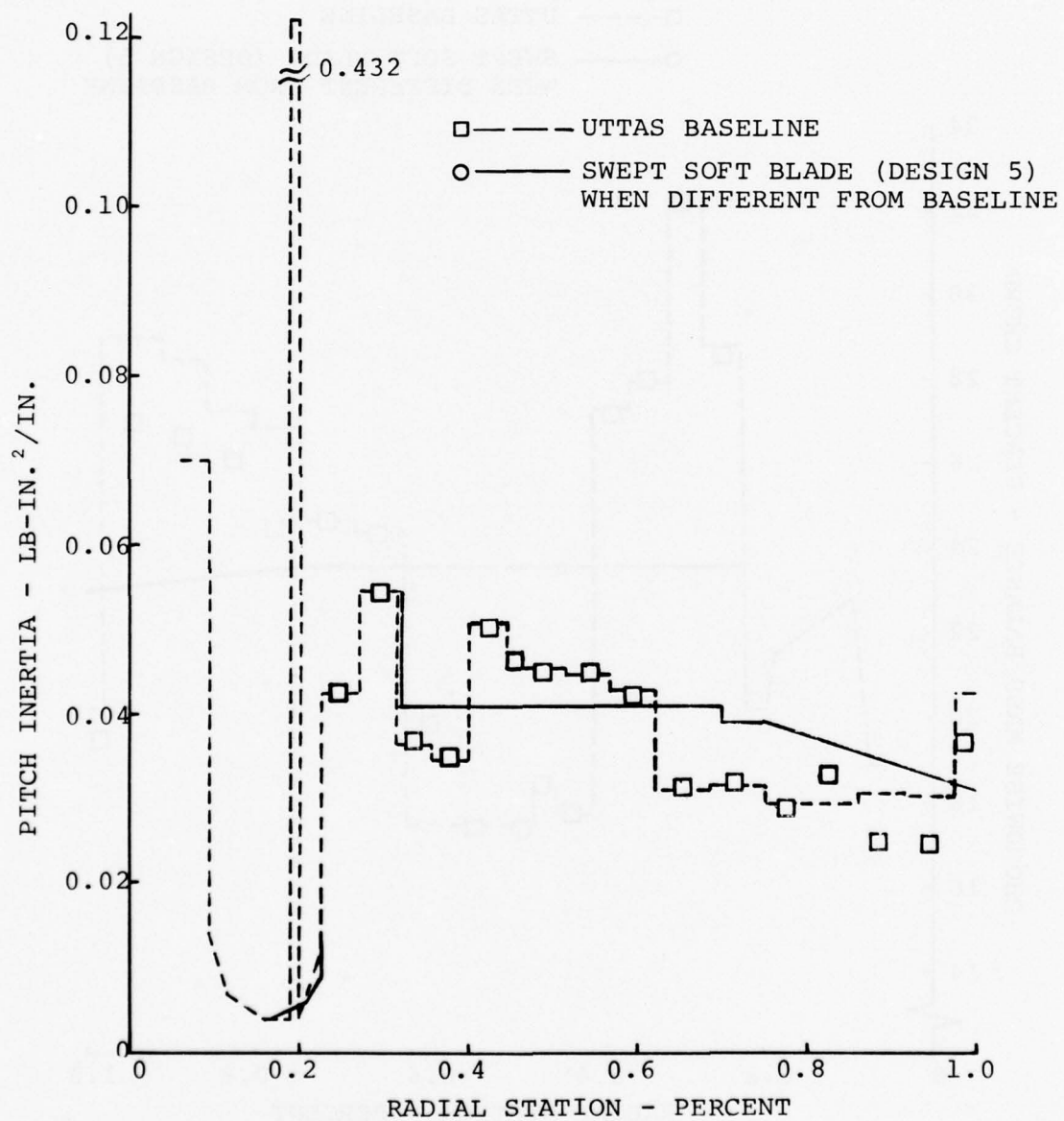


Figure 2. Comparison of Blade Properties (Sheet 3 of 8).

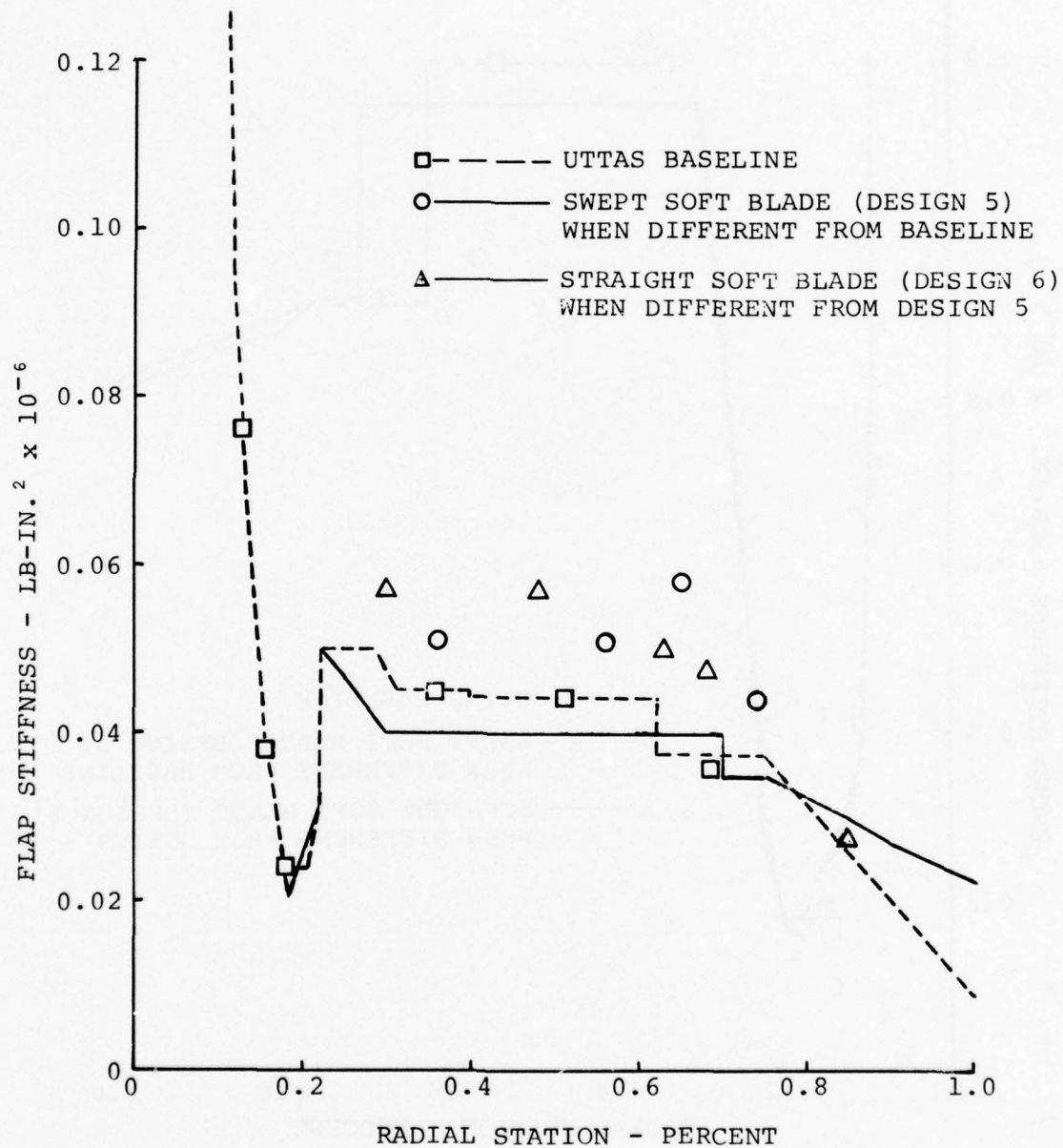


Figure 2. Comparison of Blade Properties (Sheet 4 of 8).

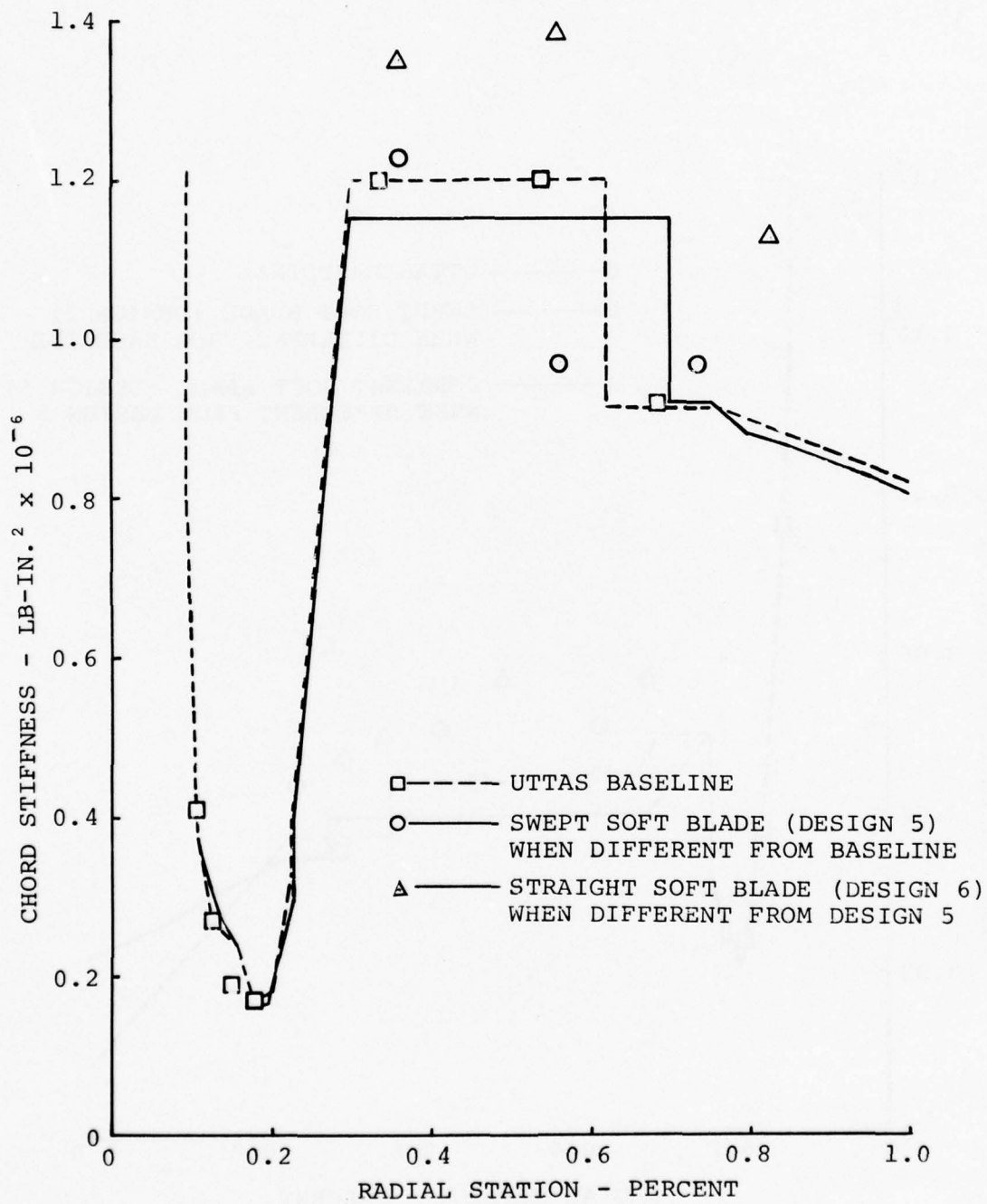


Figure 2. Comparison of Blade Properties (Sheet 5 of 8).

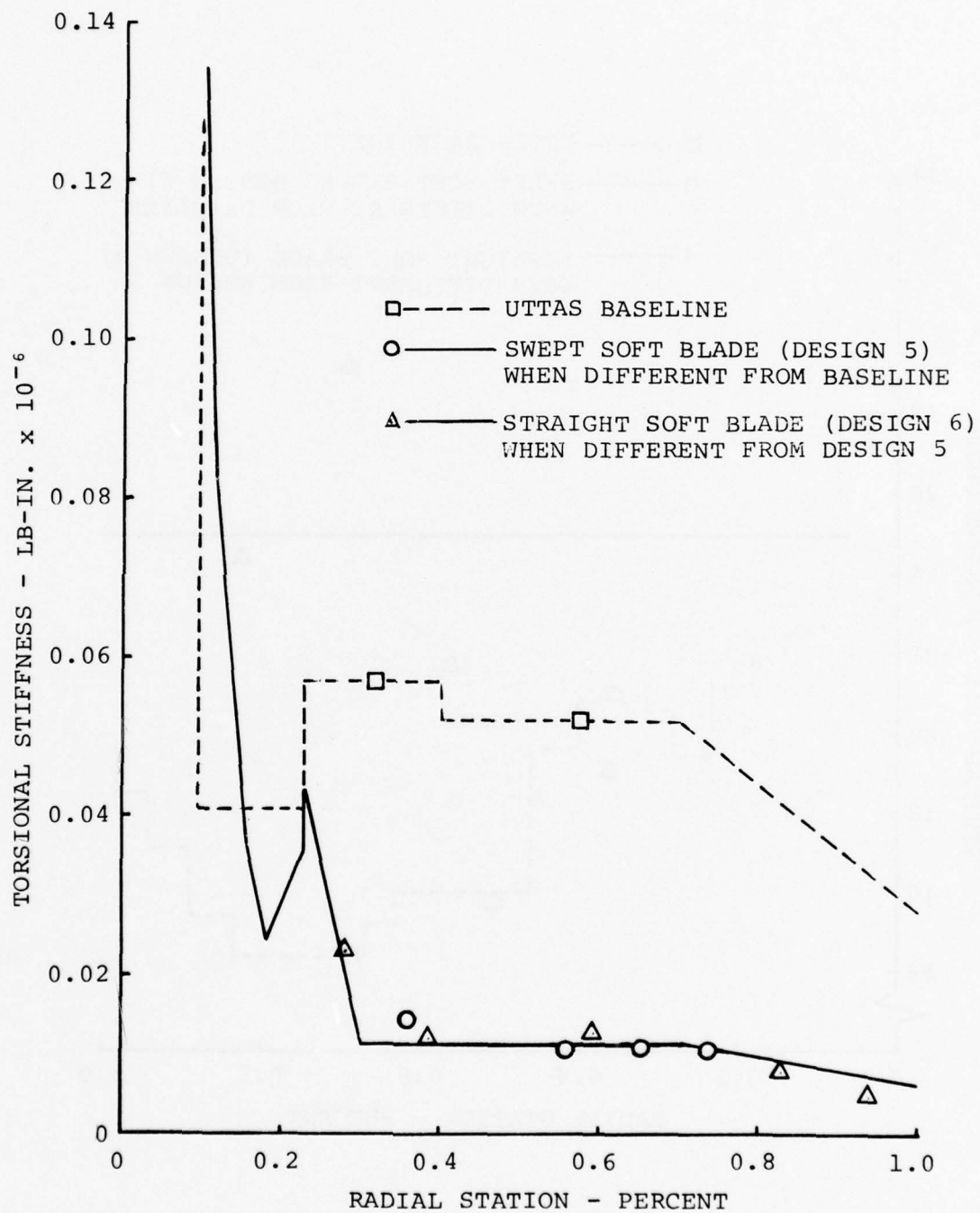


Figure 2. Comparison of Blade Properties (Sheet 6 of 8).

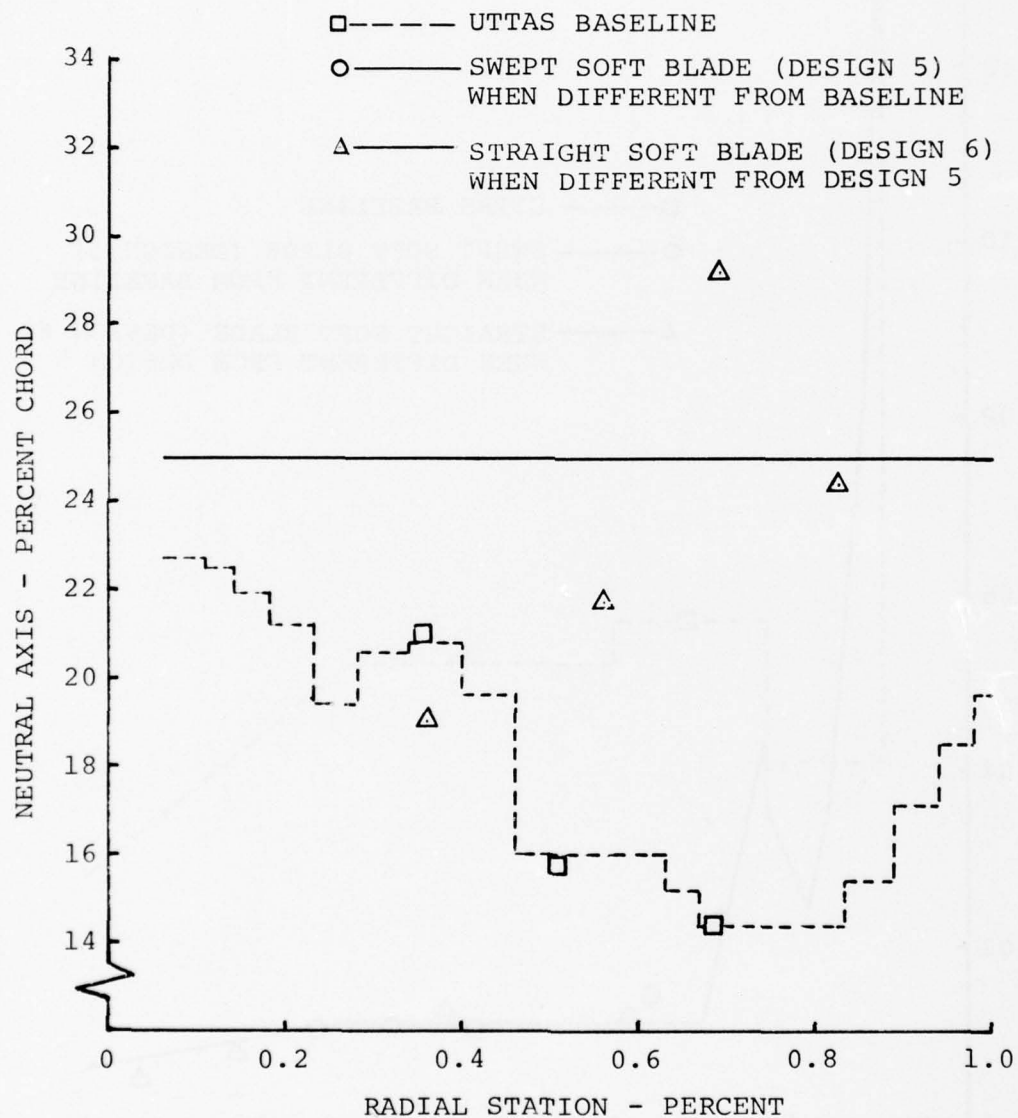


Figure 2. Comparison of Blade Properties (Sheet 7 of 8).

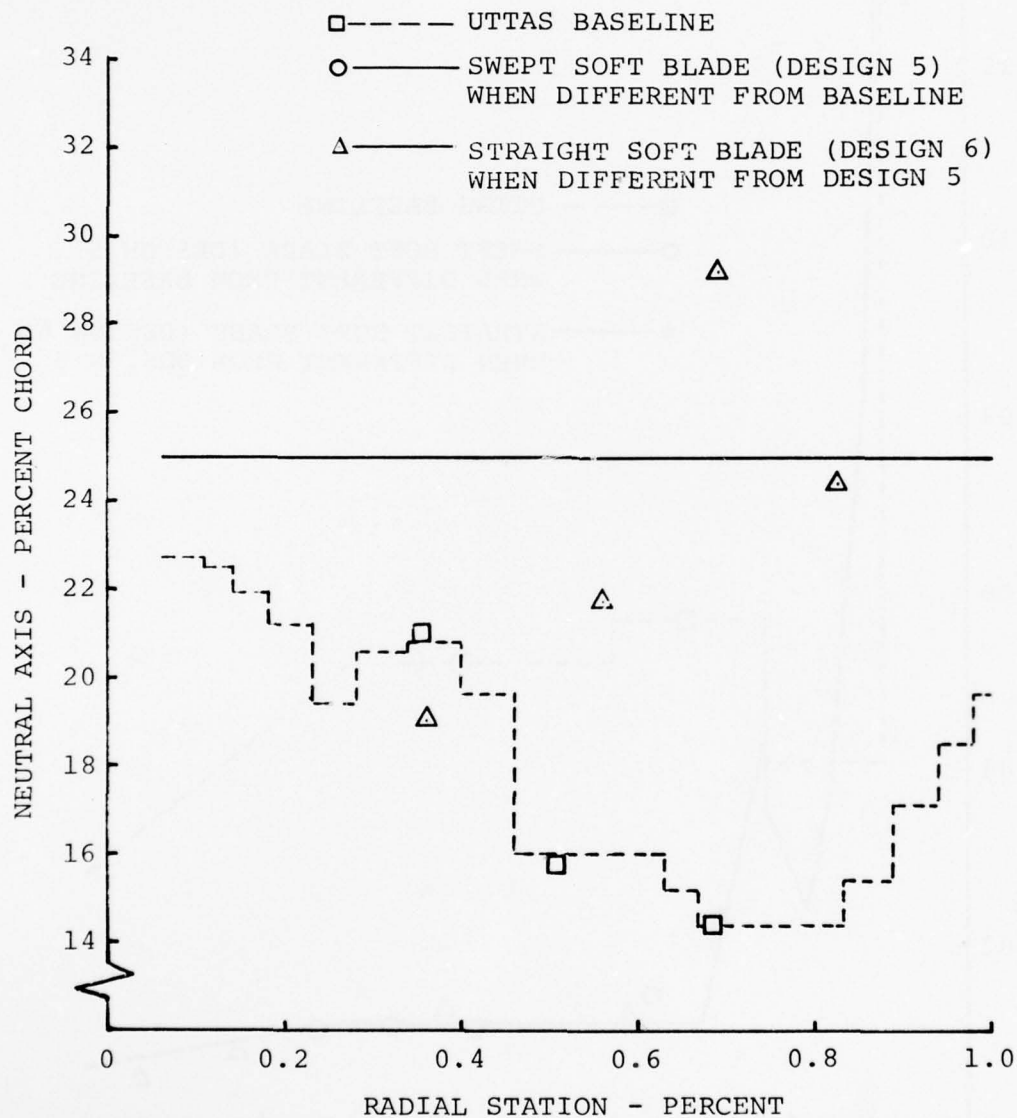


Figure 2. Comparison of Blade Properties (Sheet 7 of 8).

SHEAR CENTER

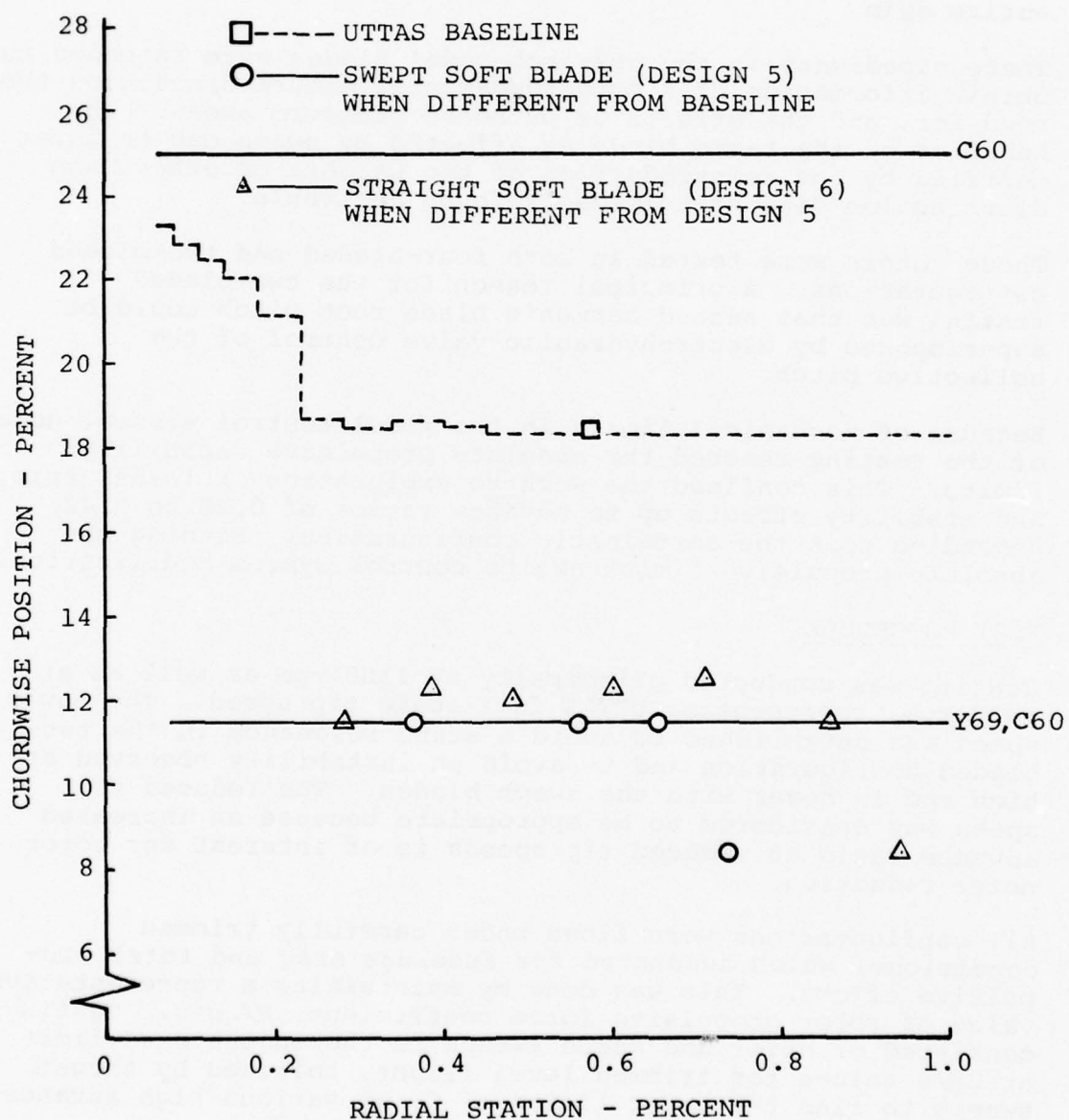


Figure 2. Comparison of Blade Properties (Sheet 8 of 8).

expected to be seen unmasked by flap bending effects due to slugged blade tips or other mass concentrations along the span. For these reasons the spanwise mass distribution of the test blades was made as uniform as possible. The elemental chordwise balance was also made as perfect as possible along the entire span.

These expedients in the research model blades were intended to obtain information of a more fundamental nature concerning the need for, and the effects of outboard planform sweep. The behavior of the basic blade as affected by sweep can be later modified by the reintroduction of tip weights or other mass distribution discontinuities if found desirable.

These rotors were tested in both four-bladed and two-bladed configurations. A principal reason for the two-bladed testing was that second-harmonic blade root pitch could be superimposed by electrohydraulic valve control of the collective pitch.

Because of mechanical limits in the model control system, none of the testing reached the absolute propulsive capability limits. This confined the work to exploration of loads, trim, and stability effects up to advance ratios of 0.28 to 0.42, depending upon the aeroelastic configuration. Finding the absolute propulsive limits awaits control system modification.

TEST PROCEDURE

Testing was conducted principally at 1100 rpm as well as at 1432 rpm, representing UTTAS full-scale tip speed. The lower speed was established to avoid a stand resonance in the two-bladed configuration and to avoid an instability observed at high rpm in hover with the swept blades. The reduced tip speed was considered to be appropriate because an increased advance ratio at reduced tip speeds is of interest for rotor noise reduction.

All configurations were flown under carefully trimmed conditions, which accounted for fuselage drag and total propulsive effort. This was done by maintaining a representative value of rotor propulsive force coefficient, $X/qd^2\sigma$. Testing consisted of hover and speed sweeps to the encountered limit at C_T/σ values for trimmed level flight, followed by thrust sweeps to find the upper limits of C_T at various high advance ratios. Testing limits are shown in Figure 3.

Extensive use was made of harmonic analysis and on-line data plotting through an IBM 1800 data processor, to study the effects of aeroelastic changes and to guide the conduct of the tests. Digital display from the data processor was used to set up the trim conditions manually for each data point.

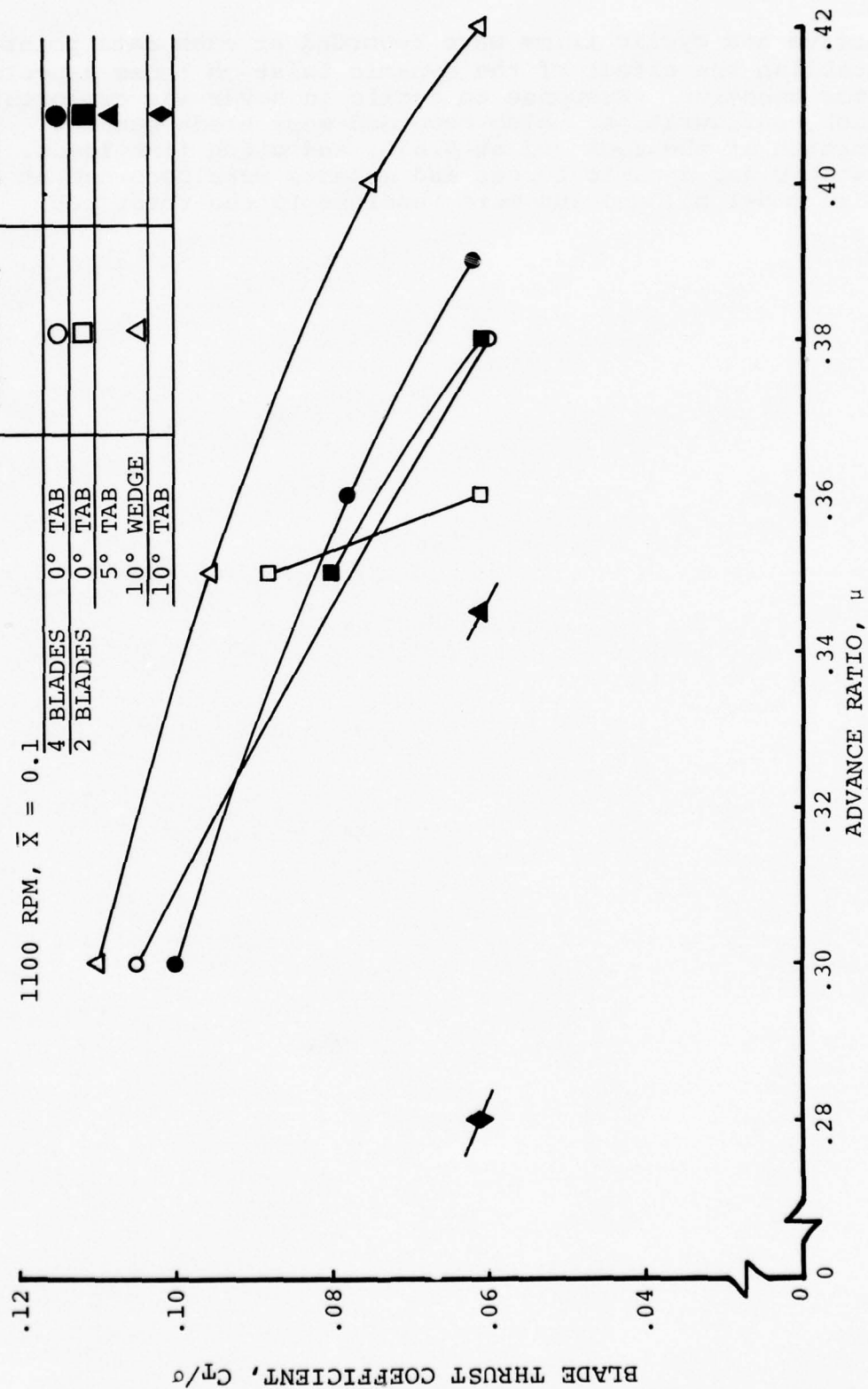


Figure 3. Wind Tunnel Test Envelope Imposed by Model Control System Limitations.

Collective and cyclic trims were recorded at each data point to establish the effect of the dynamic twist on those aspects of rotor behavior. Response to cyclic in hover was explored for each configuration. Also recorded were blade bending and torsion at the root and at 0.65R, and pitch link loads. Both static and dynamic forces and moments were recorded at the main model balance and were resolved to the rotor hub.

OBSERVED EXPERIMENTAL RESULTS

HARMONIC CONTENT OF DATA

Because the observed effects upon loads are of more interest for their harmonic content and phases than for the peak-to-peak values, the data is most profitably examined after harmonic analysis. The effects upon pitch settings required for trim are most meaningful when considered in terms of their phases. Data presented in harmonically analyzed form also facilitates the project technique of learning to control the loadings harmonic-by-harmonic with the intention of later re-assembling the desirable effects in an improved rotor design.

The combined vibratory loads in the model were constantly monitored and did not become a limit on operation in any regime of interest. This resulted in part from the fact that a project objective is to suppress vibratory loads at high advance ratio.

Amplitudes of induced torsional deflection in the blades were those attained when the forcing mechanisms acted upon the lowered blade torsional stiffness. That stiffness was the minimum which could be easily achieved in a reasonably rugged blade. Control system stiffness was left unchanged. The resulting first mode torsional frequency, ω_t , was about 3.3Ω at 1100 rpm for both the straight and swept blades.

Highlights of the test results may be best examined by separating the effects derived from the two imposed sources of dynamic twist (aerodynamic pitching moment and sweep) and from the effects of applying second-harmonic blade root pitch.

EFFECTS OF PITCHING MOMENT COEFFICIENT, C_{M_0}

The straight planform blades were subjected to changes of aerodynamic pitching moment by changing wedges attached to the trailing-edge cusp. Three configurations were tested:

- Bare cusp as molded.
- Radially varying wedges on the upper surface in a UTTAS configuration.
- Constant 10-degree wedges on the upper surface which created a ΔC_{M_0} of 0.033 along the entire span.

The swept blades were provided with a bendable cusp and were flown in three configurations:

- Bare cusp as molded
- Cusp bent upward over the entire span to obtain a ΔC_{M_0} of 0.033 (equivalent of the full span wedge effect on the straight blades)
- Cusp bent upward over the entire span to obtain a ΔC_{M_0} of 0.065.

It was known from prior experience and analysis that only positive C_{M_0} would be of interest, since both bending loads and speed stability would be adversely affected by negative C_{M_0} applied to the baseline airfoil.

C_{M_0} Changes on Straight Blades

Plotted in Figures 4 through 6 are the effects of ΔC_{M_0} upon trim, flap bending, and the rotor performance parameter L/D_E for the straight blades.

Trim -- The fact that both static and dynamic twists result from the ΔC_{M_0} is apparent from the trim data. Effective twists at 0.75R due to a ΔC_{M_0} of 0.033 are:

- 2.5 degrees steady (tip up, reducing the built-in twist) as indicated by hover collective trim.
- ± 3.6 degrees one-per-rev at $\mu = 0.36$, as indicated by cyclic trim effects.

The speed stability effect of the μ -sensitive noseup $\sin \psi$ twist derived from positive C_{M_0} reduces the flyable advance ratio limit as set by the mechanical limit of available cyclic pitch.

Although the effect of C_{M_0} on the propulsive limit could not be directly observed, its second-harmonic aspects can be deduced by examining the second-harmonic twist effects. The use of positive C_{M_0} to suppress flap bending introduced a small second-harmonic twist, about 0.4 degree (not shown in Figure 4), which peaks at $\psi = 105$ degrees and 285 degrees. This phase of second-harmonic twist tends to load the re-treating blade. Thus the C_{M_0} effects which are favorable to flap bending attenuation were, in their second-harmonic aspects, slightly unfavorable to the absolute propulsive limit.

Flap Bending -- The reduction of first- and second-harmonic outboard flap bending with ΔC_{M_0} is shown in Figure 5. The favorable effect was approximately double that seen on the swept blades where the applied ΔC_{M_0} was doubled.

TRIMMED LEVEL FLIGHT AT $C_T/\sigma = 0.06$, $\bar{X} = 0.135$, HUB MOMENT = 0
2 BLADES, 1100 RPM

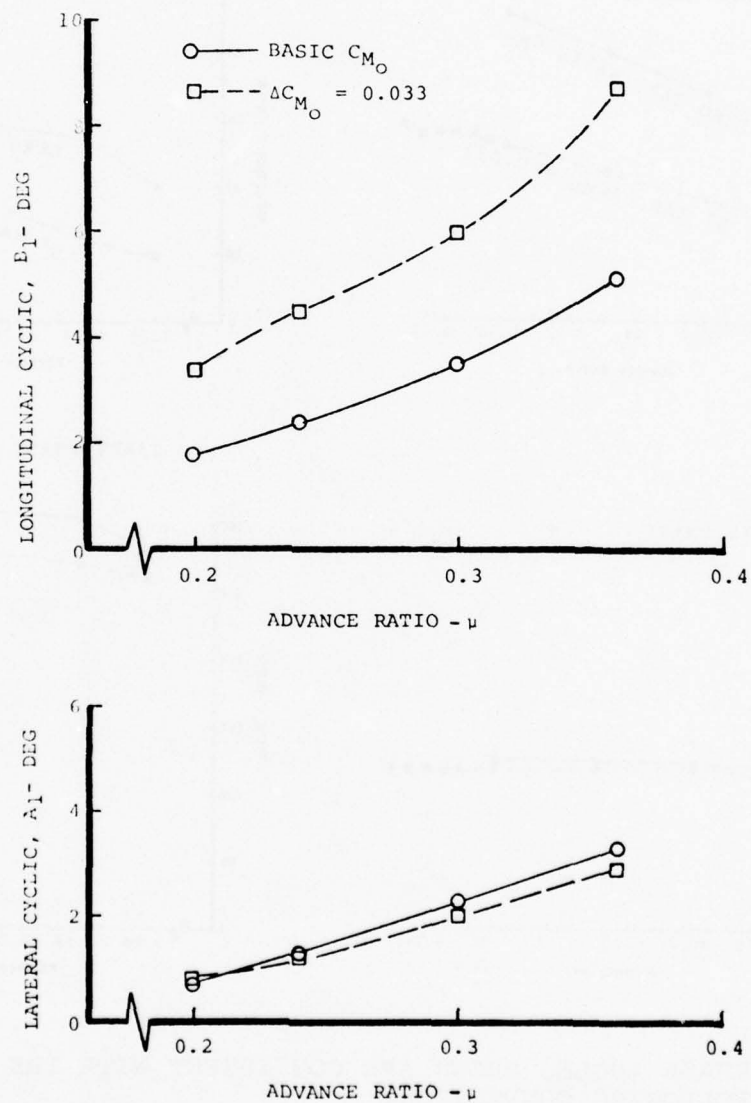
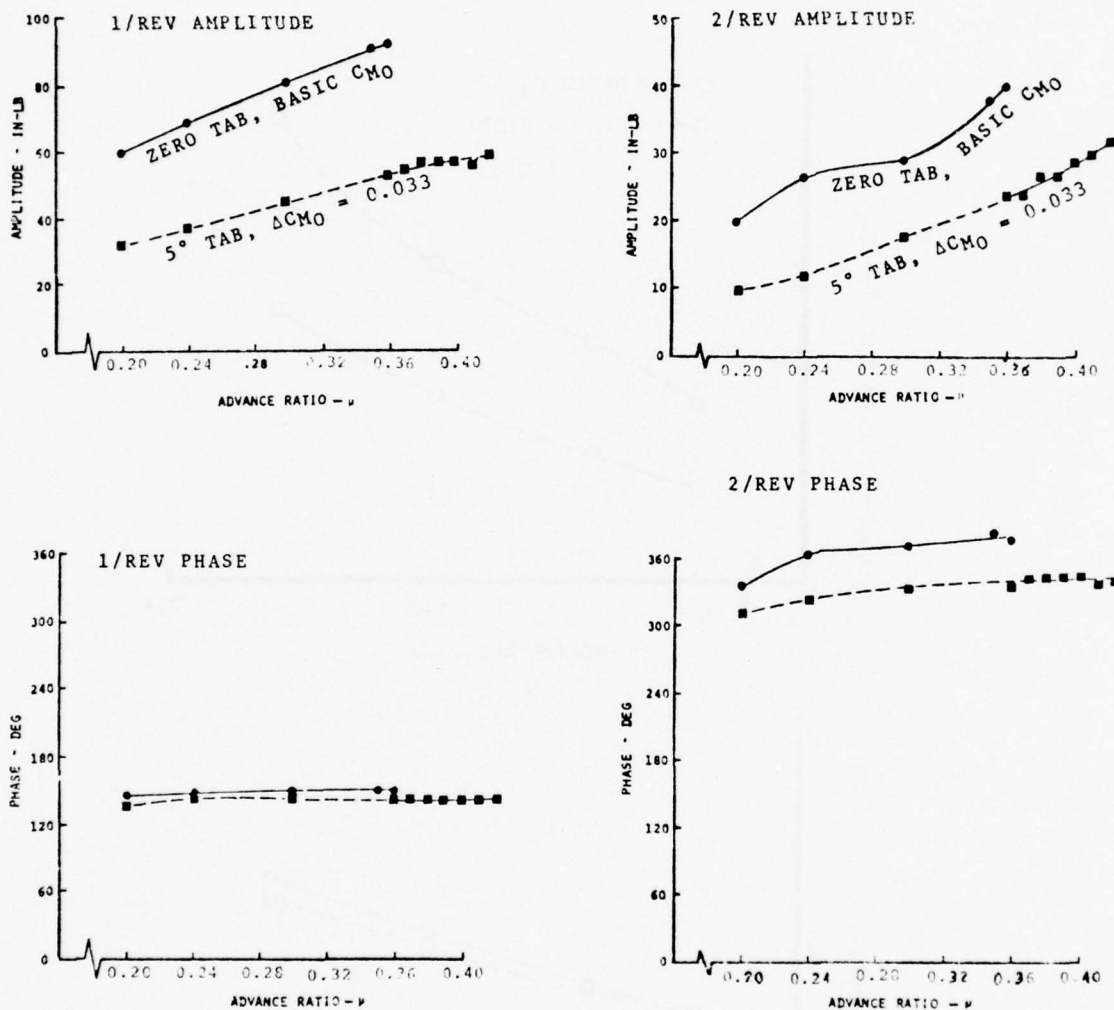


Figure 4. C_{M_O} Effect on Cyclic Trim: Straight, Soft Blade (Design 6).

TRIMMED LEVEL FLIGHT AT $C_T/\sigma = 0.06$, $\bar{X} = 0.135$, HUB MOMENT = 0
2 BLADES, 1100 RPM



PHASE ANGLES SHOWN ARE CONSISTENT WITH THE FOLLOWING CONVENTION:

$$x(\psi) = \sum_n x_n \sin(n\psi + \phi_n)$$

Figure 5. CM_O Effect on Flap Bending at 0.63 R :
Straight, Soft Blade (Design 6).

TRIMMED LEVEL FLIGHT AT $C_T/\sigma = 0.06$, $\bar{X} = 0.135$, HUB MOMENT = 0
2 BLADES, 1100 RPM

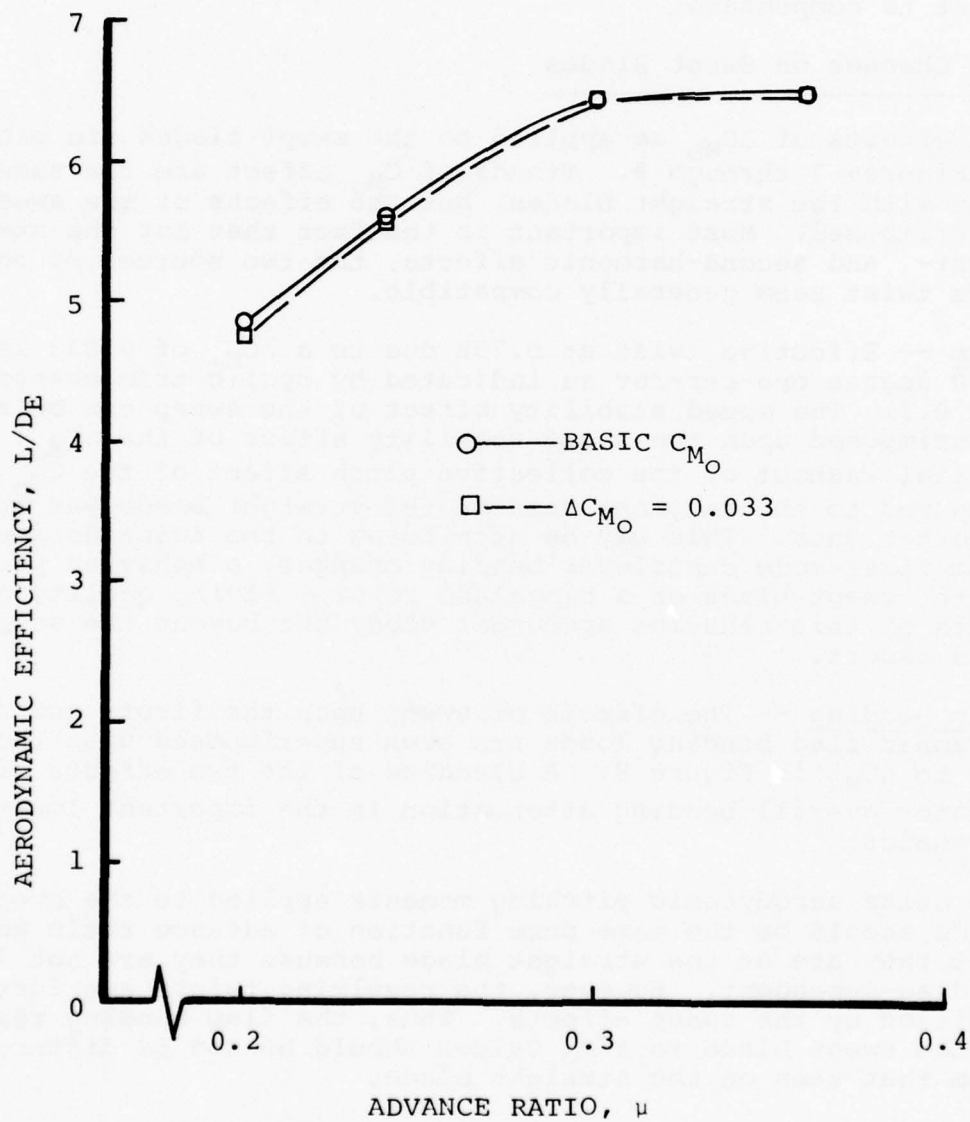


Figure 6. C_{M_O} Effect on Aerodynamic Efficiency :
Straight, Soft Blade (Design 6).

Aerodynamic Performance Parameter, L/D_E -- As indicated in Figure 6, the rotor's forward flight aerodynamic performance was not significantly affected by the changes of dynamic twist. Hover efficiency was slightly reduced because static twist was reduced by the steady noseup component of elastic twist. This would be restored by changing the as-molded design twist to compensate.

C_{M_0} Changes on Swept Blades

The effects of ΔC_{M_0} as applied to the swept blades are plotted in Figures 7 through 9. Trends of C_{M_0} effect are the same as seen with the straight blades, but the effects of the sweep are superimposed. Most important is the fact that for the steady, first-, and second-harmonic effects, the two sources of corrective twist seem generally compatible.

Trim -- Effective twist at 0.75R due to a ΔC_{M_0} of 0.033 is +1.0 degree one-per-rev as indicated by cyclic trim changes at $\bar{\mu} = 0.3$. The speed stability effect of the sweep can be seen superimposed upon the speed stability effect of the ΔC_{M_0} . A partial washout of the collective pitch effect of the C_{M_0} as compared to the response seen on the straight blade was apparent in other data. This may be attributed to the twist derived from first-mode cantilever bending changes, a behavior peculiar to the swept blade on a hingeless rotor. Flying quality aspects of this behavior are under study but beyond the scope of this report.

Flap Bending -- The effects of sweep upon the first- and second-harmonic flap bending loads are seen superimposed upon those due to ΔC_{M_0} in Figure 8. A blending of the two effects creates greater overall bending attenuation in the important lower harmonics.

The delta aerodynamic pitching moments applied to the swept blade should be the same pure function of advance ratio and C_{M_0} that they are on the straight blade because they are not lift- or drag-dependent. However, the resulting twists are further modified by the sweep effects. Thus, the flap bending response of the swept blade to ΔC_{M_0} values should be and is different from that seen on the straight blade.

Aerodynamic Performance Parameter, L/D_E -- As seen in Figure 9, the forward flight performance parameter was less favorable at high advance ratio than that seen with the straight blades. Further, the deficiency was made slightly worse when the positive C_{M_0} was combined with the sweep. These effects are further discussed in following paragraphs.

TRIMMED LEVEL FLIGHT AT $C_T/\sigma = 0.06$, $\bar{X} = 0.135$, HUB MOMENT ≈ 0
2 BLADES, 1100 RPM

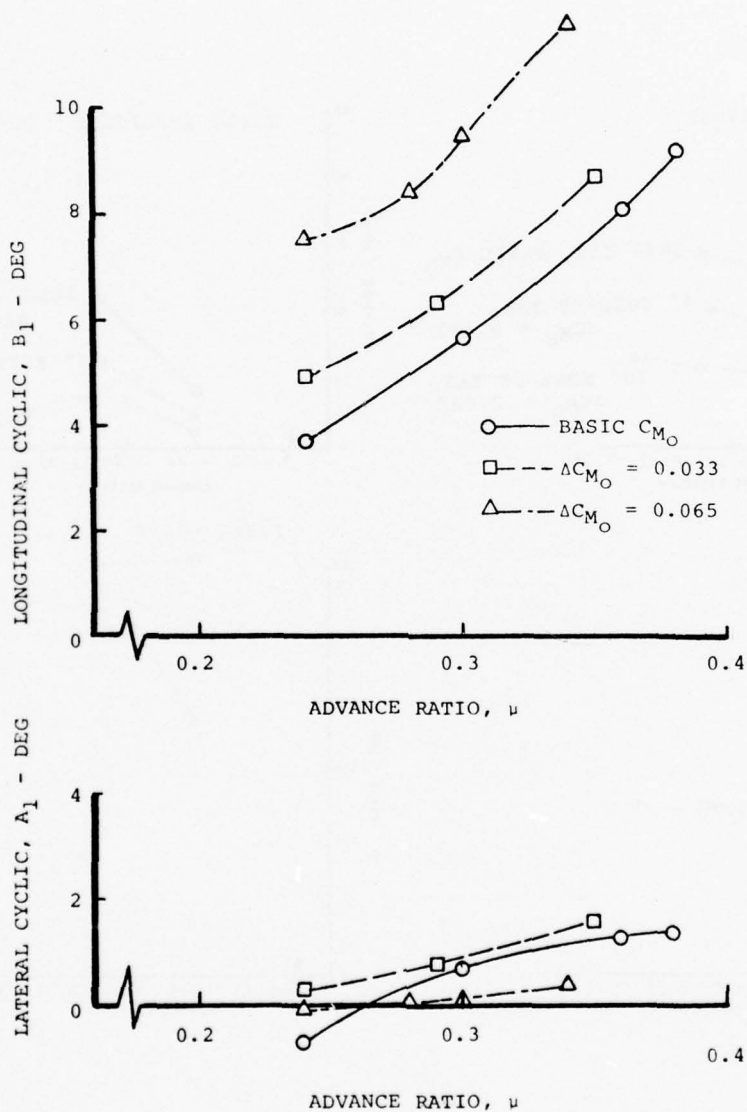


Figure 7. C_{M_O} Effect on Cyclic Trim: Swept, Soft Blade (Design 5).

TRIMMED LEVEL FLIGHT AT $C_T/\sigma = 0.06$, $\bar{X} = 0.135$, HUB MOMENT = 0
2 BLADES, 1100 RPM

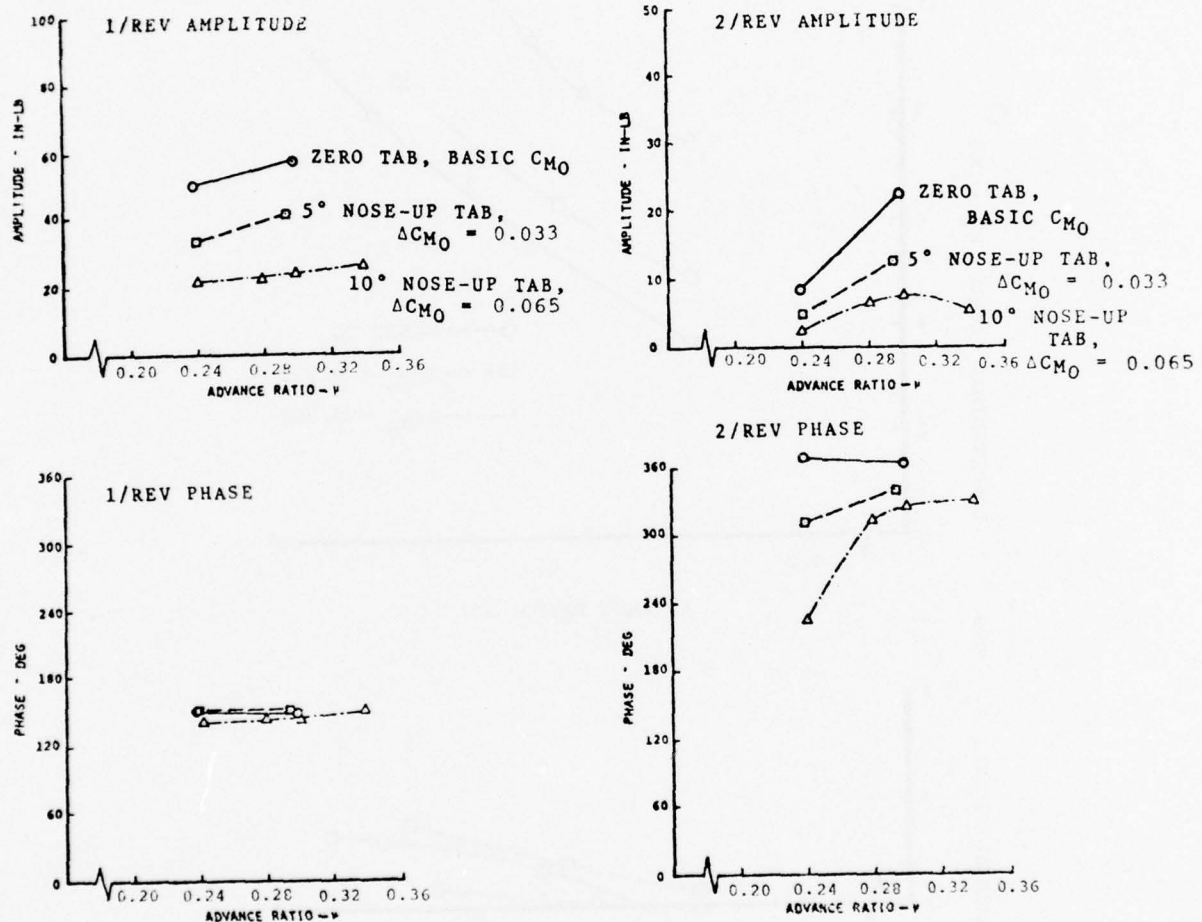


Figure 8. C_{M0} Effect on Flap Bending at 0.67R:
Swept, Soft Blade (Design 5).

TRIMMED LEVEL FLIGHT AT $C_T/\sigma \approx 0.06$, $\bar{X} = 0.135$, HUB MOMENT = 0
2 BLADES, 1100 RPM

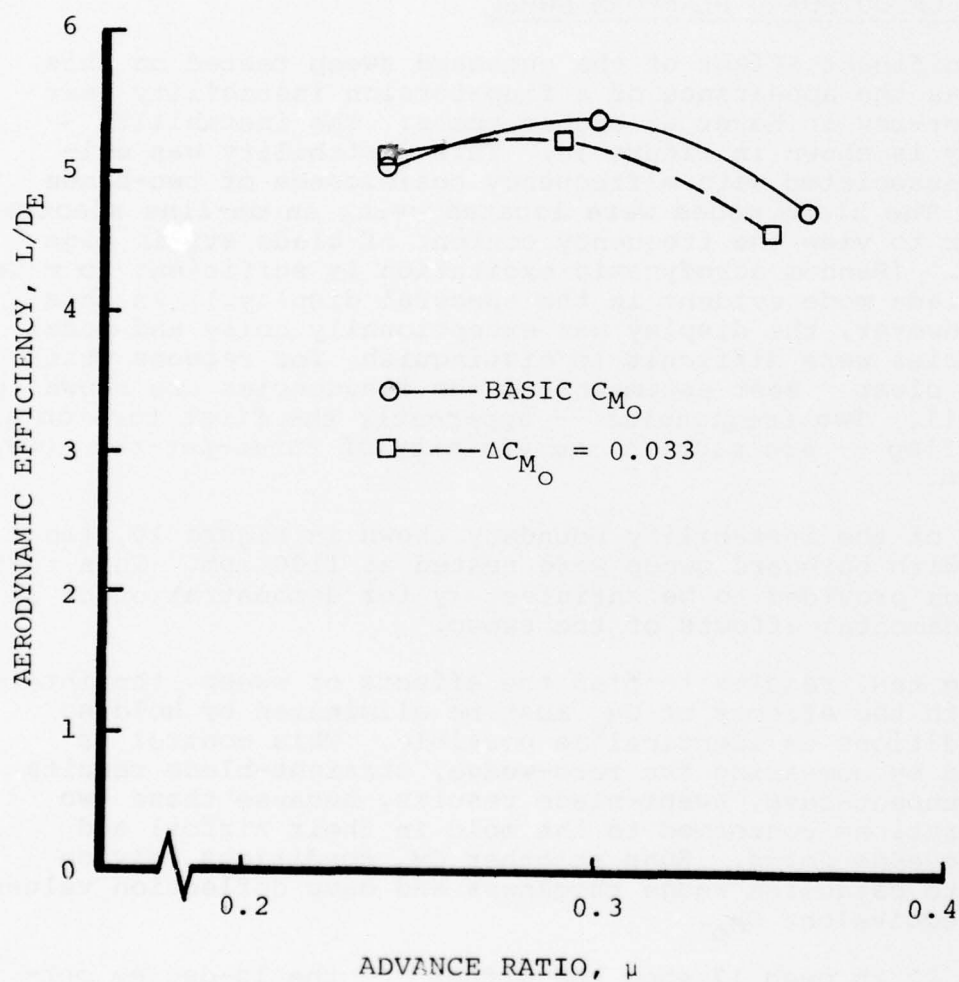


Figure 9. C_{M_O} Effect on Aerodynamic Efficiency :
Swept, Soft Blade (Design 5).

Hover efficiency of the swept blade was somewhat reduced when positive CM_0 was introduced. This effect was less, however, than seen with the straight blade, and can be reconciled with the fact that the sweep should resist the static untwisting of the blade. The net untwisting of the blade would be restored in a real blade design to regain the hover performance.

EFFECTS OF OUTBOARD PLANFORM SWEEP

One significant effect of the outboard sweep tested on this rotor was the appearance of a flap-torsion instability near three-per-rev in hover at higher rpm's. The instability boundary is shown in Figure 10. This instability was evidently associated with a frequency coalescence of two-blade modes. The blade modes were located using an on-line spectral analyzer to view the frequency content of blade strain gage signals. (Random aerodynamic excitation is sufficient to make every blade mode evident in the spectral display.) In this case, however, the display was exceptionally noisy and modal frequencies were difficult to distinguish, for reasons which are not clear. Best estimates of the frequencies are shown in Figure 11. Two frequencies -- apparently the first torsion and second flap -- are seen in the vicinity of three-per-rev above 1000 rpm.

Because of the instability boundary shown in Figure 10, the blades with outboard sweep were tested at 1100 rpm. This test condition provided to be satisfactory for demonstration of all the fundamental effects of the sweep.

In using test results to find the effects of sweep, the interplay with the effects of CM_0 must be eliminated by holding CM_0 conditions as identical as possible. This control is provided by comparing the zero-wedge, straight-blade results to the unbent-cusp, swept-blade results, because these two configurations conformed to the mold in their airfoil and trailing-edge forms. Runs at other CM_0 conditions rely on theory to establish wedge thickness and cusp deflection values giving equivalent CM_0 .

Figures 12 through 17 show the effects of the 10-degree outboard planform sweep upon trim, flap bending, and the rotor performance parameter L/D_E . The effects upon absolute propulsive limit will be discussed but were not directly revealed in the data.

Trim -- The root collective pitch required to obtain an increment of thrust is about 38 percent greater for the swept blade, due principally to the washout of outboard pitch by torsion resulting from incremental first mode flap bending.

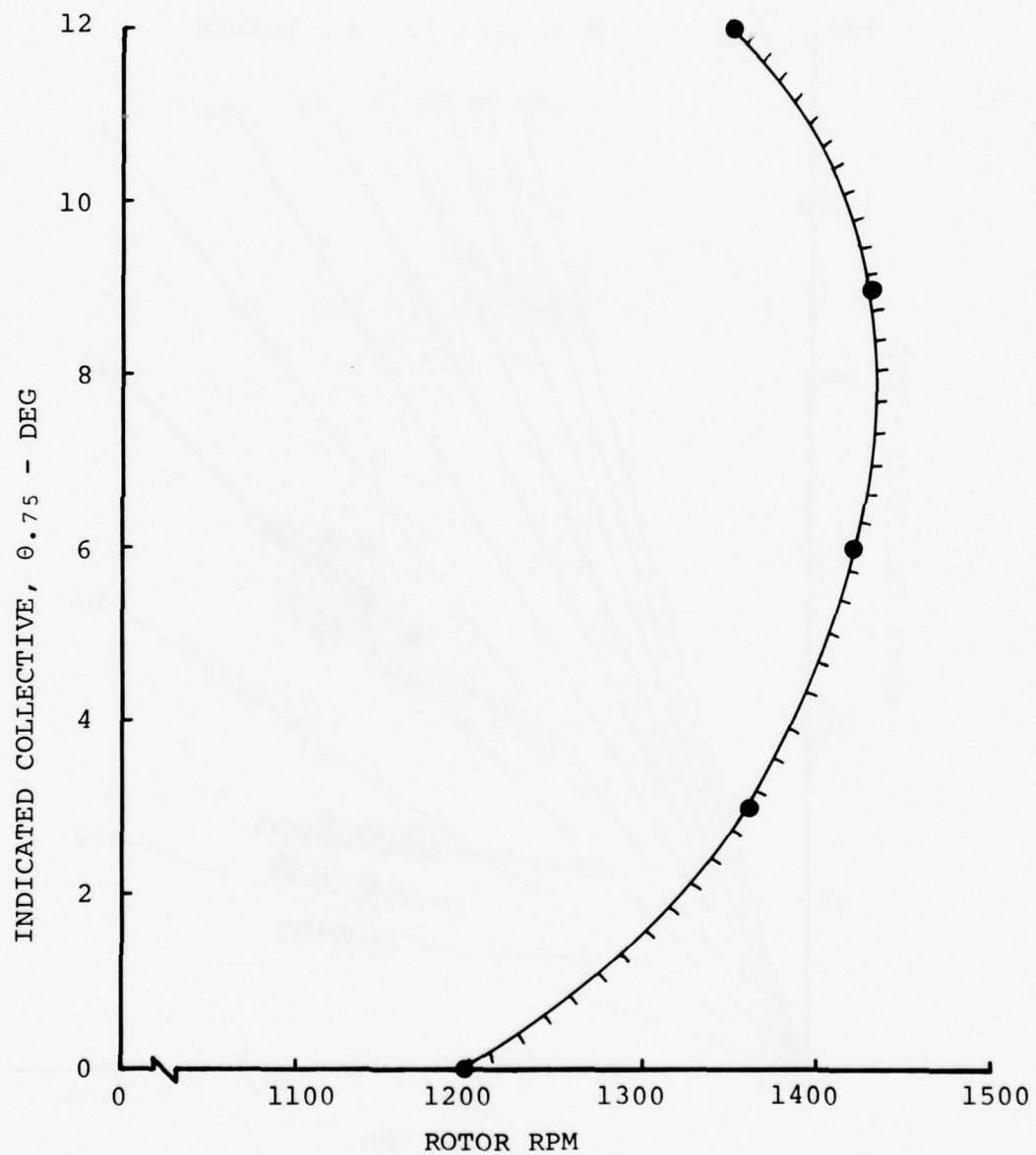


Figure 10. Aeroelastic Stability Limits of Swept, Soft Blades (Design 5).

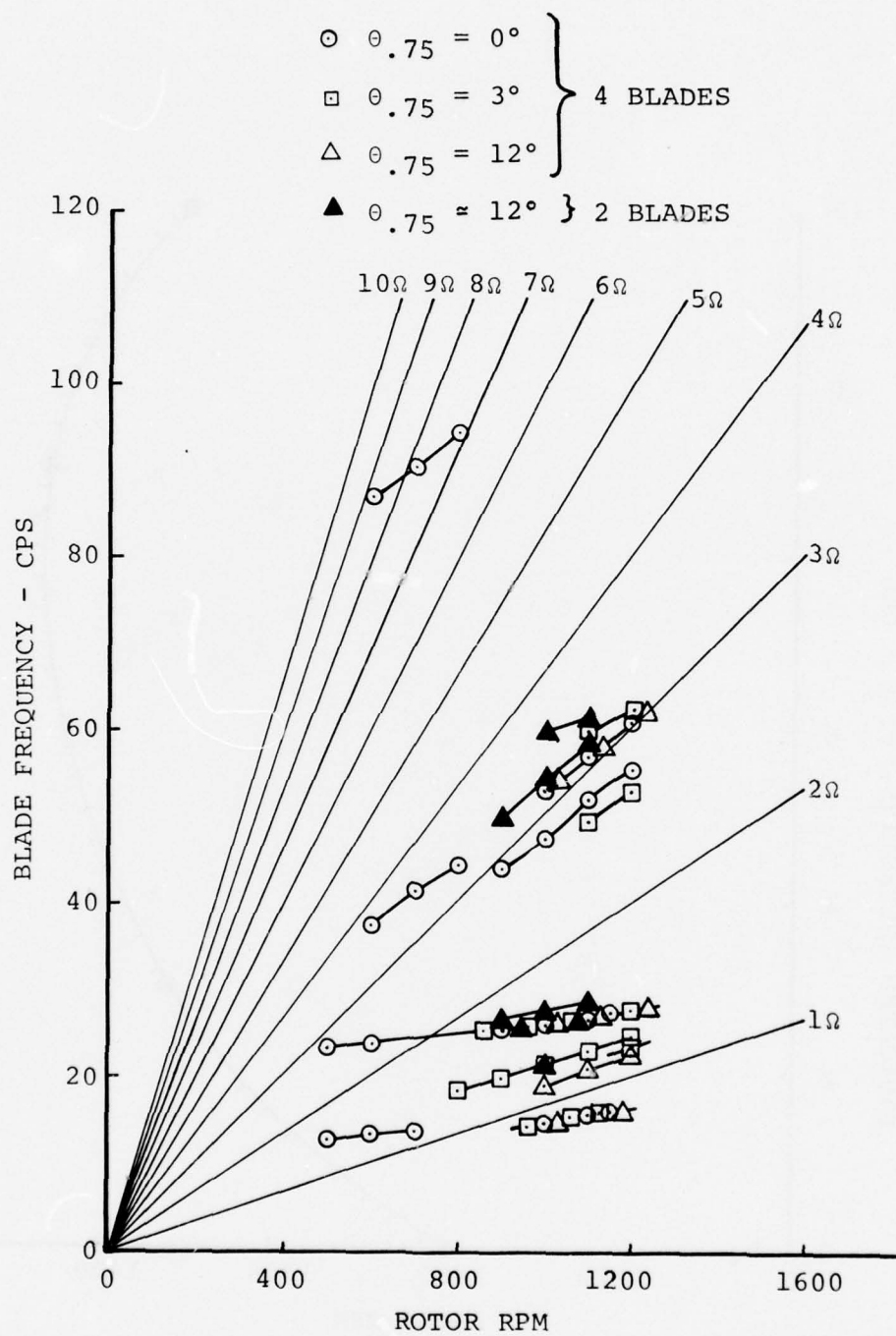


Figure 11. Modal Frequencies Observed with On-Line Spectral Analyzer: Swept, Soft Blades (Design 5).

TRIMMED LEVEL FLIGHT AT $C_T/\sigma = 0.06$, $\bar{X} = 0.135$, HUB MOMENT = 0
2 BLADES, 1100 RPM

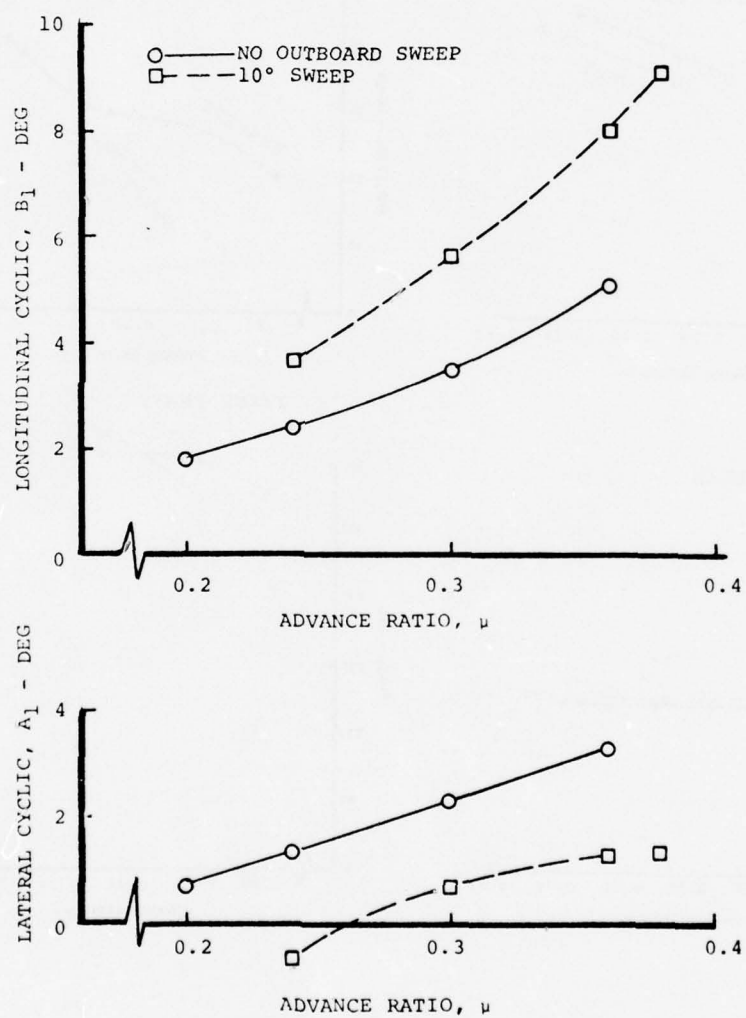


Figure 12. Outboard Sweep Effect on Cyclic Trim: Zero Tab

TRIMMED LEVEL FLIGHT AT $C_{T/\sigma} = 0.06$, $\bar{X} = 0.135$, HUB MOMENT = 0
2 BLADES, 1100 RPM

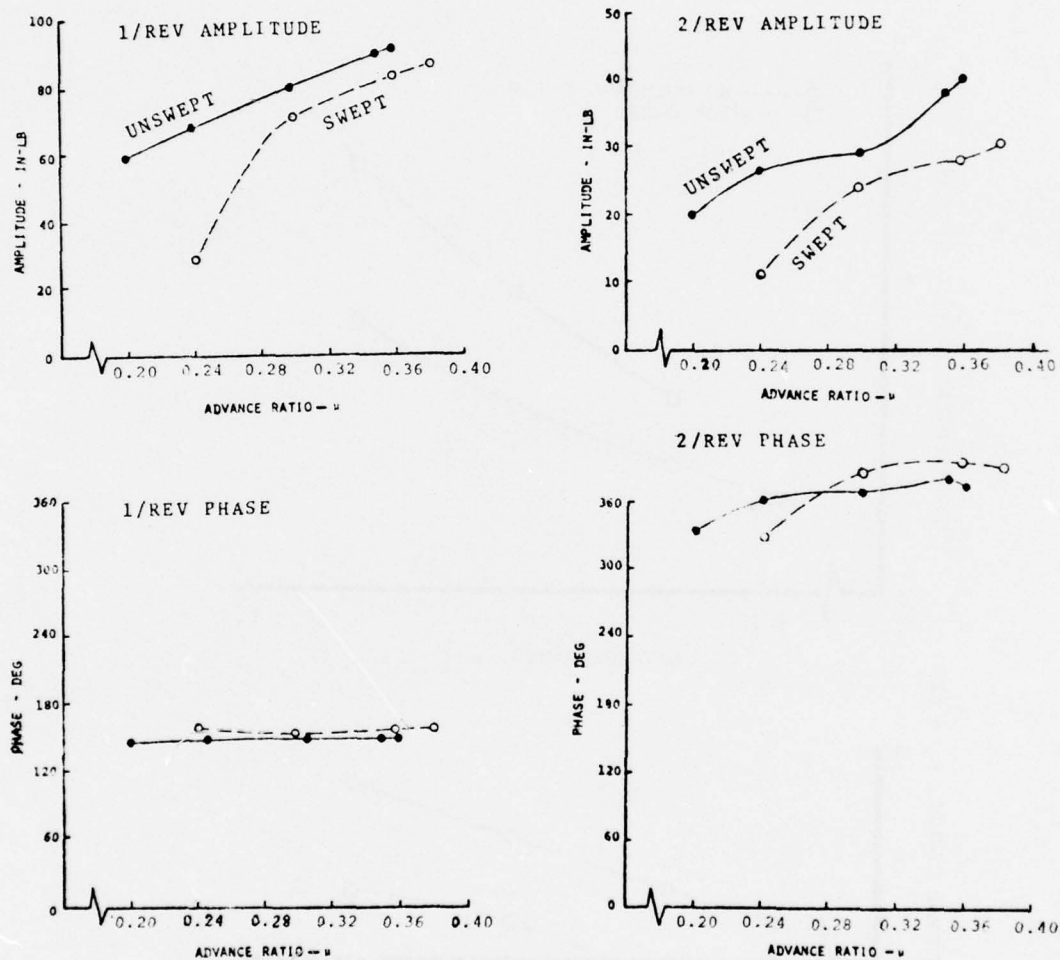


Figure 13. Outboard Sweep Effect on Flap Bending at 0.63R : Zero Tab.

TRIMMED LEVEL FLIGHT AT $C_T/\sigma = 0.06$, $\bar{X} = 0.135$, HUB MOMENT = 0
2 BLADES, 1100 RPM

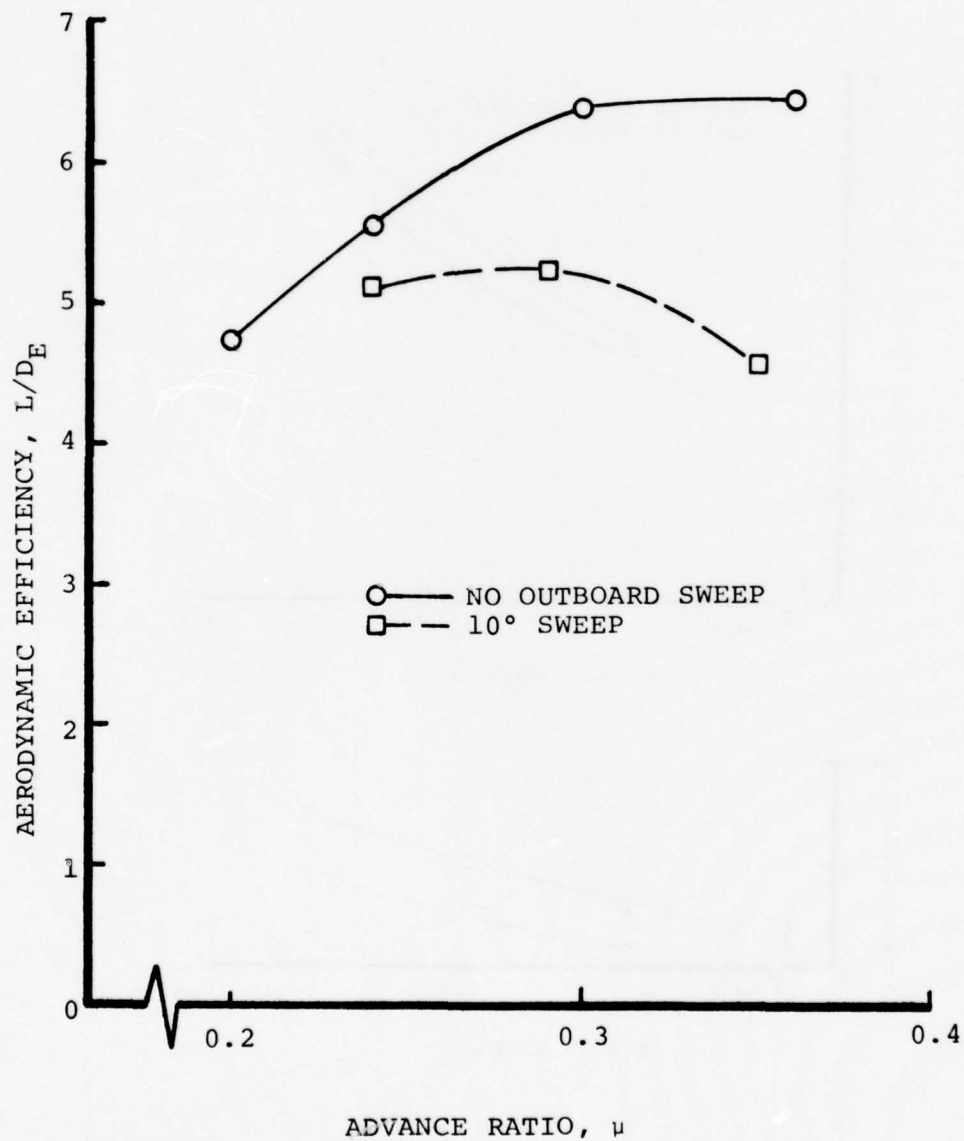


Figure 14. Outboard Sweep Effect on Aerodynamic Efficiency:
Zero Tab.

TRIMMED LEVEL FLIGHT AT $C_T/\sigma = 0.06$, $\bar{X} = 0.135$, HUB MOMENT = 0
2 BLADES, 1100 RPM

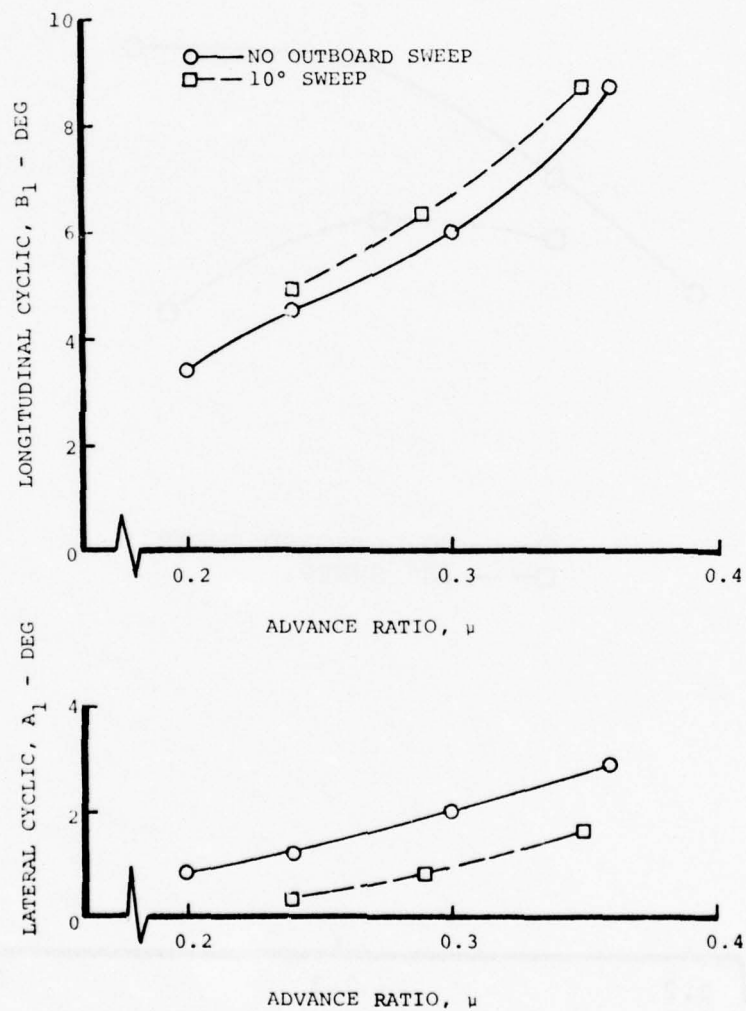


Figure 15. Outboard Sweep Effect on Cyclic Trim:
 $\Delta C_{M_0} = 0.033$

TRIMMED LEVEL FLIGHT AT $C_T/\sigma = 0.06$, $\bar{X} = 0.135$, HUB MOMENT = 0
2 BLADES, 1100 RPM

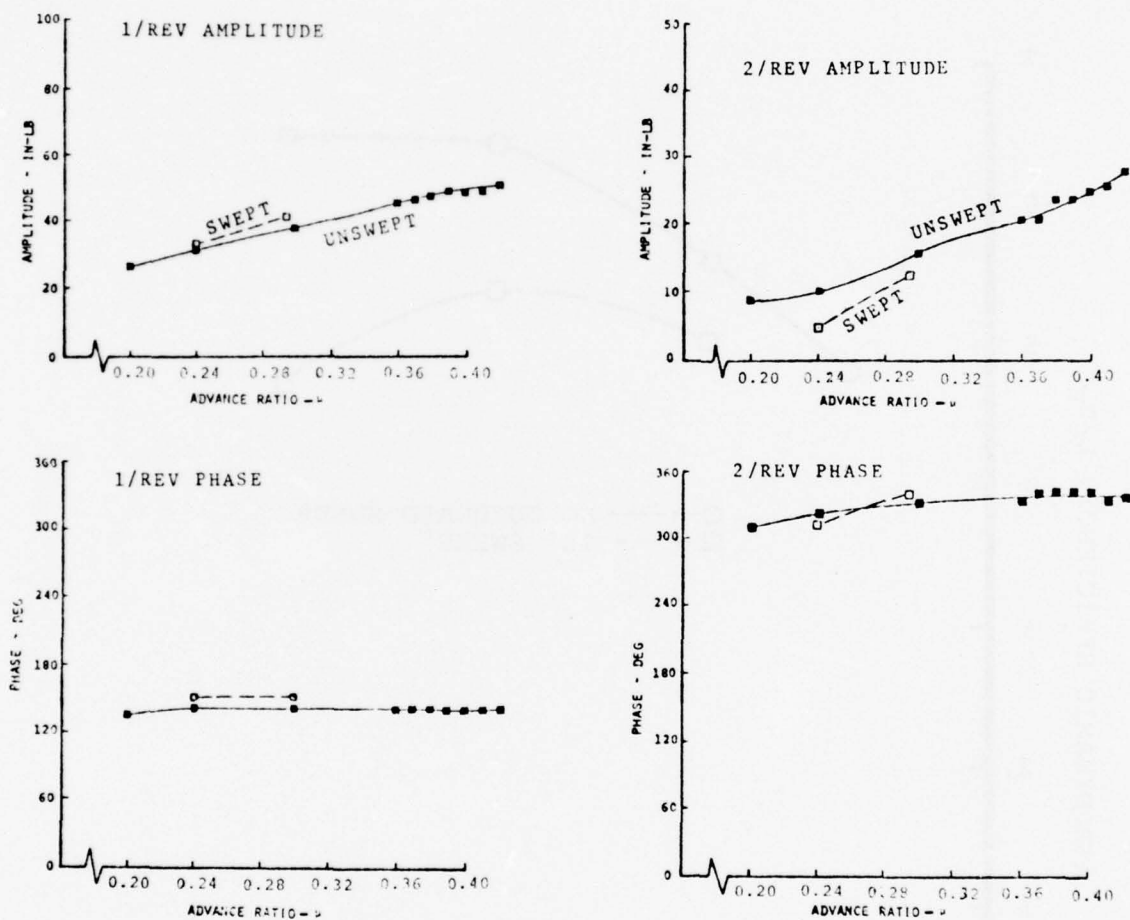


Figure 16. Outboard Sweep Effect on Flap Bending at
0.067R: $\Delta C_{M_0} = 0.033$.

TRIMMED LEVEL FLIGHT AT $C_T/\sigma = 0.06$, $\bar{X} = 0.135$, HUB MOMENT = 0
2 BLADES, 1100 RPM

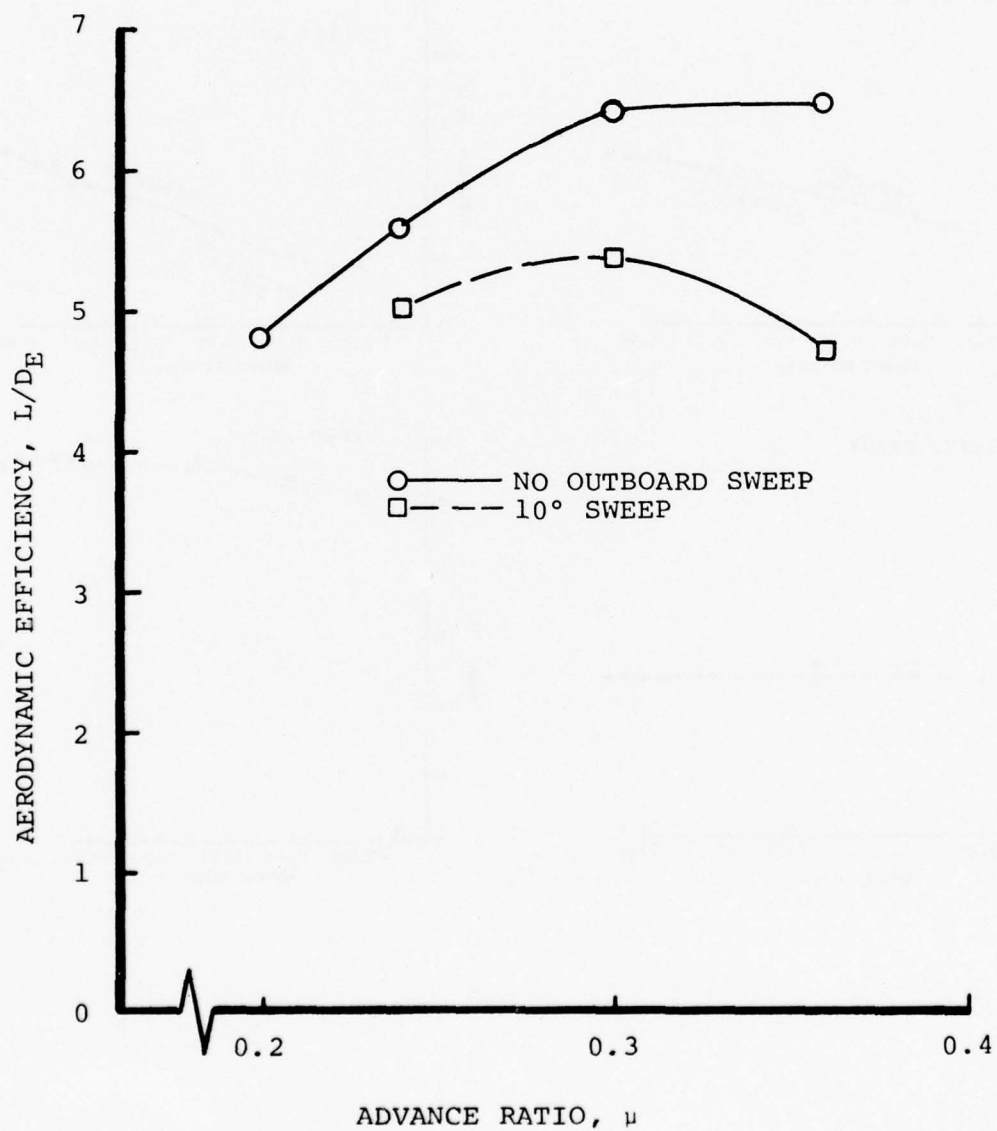


Figure 17. Outboard Sweep Effect on Aerodynamic Efficiency:
 $\Delta C_{M_0} = 0.033$

This effect is peculiar to a hingeless or teetering rotor and largely absent from a fully articulated system.

The amplitude of root cyclic pitch required to obtain an increment of shaft moment in hover was not changed by sweep, but the cyclic pitch was input at a different azimuth to obtain the same shaft moment.

There is a speed-stabilizing cyclic twist effect which arises from the sweep, coupled with the fact that second-mode flap bending at one-per-rev tends to develop with advance ratio. This bending is tip down at $\psi = 90$ degrees, thus the sweep-induced twist is noseup near 90 degrees. As shown in Figure 11, this sweep effect increased by 3.0 degrees the forward cyclic required to trim the zero tab blade at $\mu = 0.36$.

Sweep Effects on Propulsive Capability Limit -- It can be reasoned that the first-harmonic twist caused by the sweep and seen in the trim data is of a phase which should be detrimental to the absolute propulsive limit. The reasoning is that there is increased nosedown twist at $\psi = 270$ degrees and that the cyclic used to compensate will therefore increase the pitch of the inboard retreating blade region. The reverse flow should, in turn, create increased downloads and contribute to earlier deterioration of the propulsive capability.

Although not seen directly in the trim data, there is also a second-harmonic twist induced by the sweep which should affect the propulsive limit. Study of the blade torsion data shows that this second-harmonic twist is noseup at $\psi = 130$ degrees and 310 degrees. This phase is unfavorable to the $\cos 2\psi$ thrust, so this effect of the sweep should also be detrimental to the propulsive limit.

Sweep Effects on Flap Bending -- The reduction of first- and second-harmonic outboard flap bending as a result of the introduction of sweep is shown in Figures 13 and 16. The bending attenuation is created by the sweep as a coupler of torsion to bending and is seen to be greatest in the comparison of the no-wedge straight blade to the unbent-cusp swept blade. Because the favorable noseup ΔC_{M_0} effect was absent, the initial flap bending was high. Thus the bending moment available to the sweep coupling was large and its absolute effects were large.

For the blades with $\Delta C_{M_0} = 0.033$, Figure 16, the flap bending attenuation at the first harmonic by sweep is seen to be small and slightly negative. This conforms to theory in that the bending moment available to the sweep coupling had been reduced to the vicinity of zero by the effect of C_{M_0} .

Second-harmonic outboard bending attenuation by the sweep alone reached approximately 30 percent at $\mu = 0.3$. A greater torsional response to second-harmonic moment occurs because of the closeness of the first mode torsional natural frequency at 3.3Ω . This in turn enables the sweep to create greater bending attenuation at second harmonic than at first.

As discussed earlier, under "Trim," the phase of the second-harmonic twist generated by the sweep coupling was such that it would be unfavorable to the propulsive limit.

Sweep Effects on Aerodynamic Performance Parameter L/D_E -- The third-harmonic twist changes introduced by the outboard planform sweep created unfavorable effects upon the aerodynamic performance parameter L/D_E as partly shown in Figures 14 and 17. The first- and second-harmonic components of the twist induced by the sweep are of a character which should have improved performance, but their benefits were masked by power losses believed to be associated with stall.

Above $\mu = 0.2$, where the straight blade begins to show signs of stall, the swept blade starts a more rapid decay of L/D_E and by $\mu = 0.3$ it has peaked, falling thereafter. Study of the torsional and bending data indicates that the swept blade develops unusually large 3-per-rev torsional amplitude, which increases rapidly with μ after the first signs of stall. This large torsional oscillation, which could account for a falloff of L/D_E , appears to be a stall-forced response of the lightly damped, coupled, first-torsion second-flap mode near its natural frequency of 3.28Ω . The 3-per-rev torsion problem is an adverse feature of the particular frequency map of these blades which must be eliminated by slightly increasing the blades torsional stiffness before testing can probe the basic L/D_E of the swept-blade system.

EFFECTS OF SECOND-HARMONIC ROOT PITCH

The present interest in second-harmonic pitch control applied at the blade root lies in its potential for moving the absolute propulsive capability limit to higher values of C_T/σ at higher advance ratios. Because the limits in question could not be reached within the control ranges of the model used in these tests, the effects of second-harmonic control were only partly explored. By applying $\cos 2\psi$ pitch to the root of the straight, low torsional stiffness blades, the effects upon trim, flap bending, and L/D_E were explored at $C_T/\sigma = 0.06$ and $\mu = 0.30$, in a two-bladed version of the test rotor.

Limitations of hydraulic pressure available to the control servos held the collective pitch available at second harmonic to ± 0.35 degree. Phase of the input pitch was carefully adjusted to obtain an almost perfect $\cos 2\psi$ function as

measured at the blade root. Refined theory and future experiments will define, near the $\cos 2\psi$ phase, the exact optimum phase for propulsive augmentation.

The test data, obtained at the maximum available two-per-rev amplitude (0.35 degree), showed the following results:

Trim -- Collective trim settings are reduced by 0.75 degree per degree of $\cos 2\psi$ pitch while forward cyclic is decreased by 0.5 degree per degree of $\cos 2\psi$ pitch. These relationships qualitatively confirm simple theoretical expectations and seem more accurate in quantity than might be expected in view of the small input amplitude available.

Flap Bending -- The influence of $\cos 2\psi$ pitch upon flap bending was found to be small and not indicative that any structural problems were being introduced. This promising situation could reverse in other flight regimes and needs further scrutiny.

A study of the torsional strain data indicated that despite the low blade torsional stiffness the $\cos 2\psi$ pitch was being delivered largely undiminished to the outboard blade. This is another promising indication that the use of second-harmonic root pitch may be compatible with the other requirements of good rotor behavior.

Aerodynamic Performance Parameter L/D_E -- There was no significant change of the aerodynamic efficiency as indicated by L/D_E change when the $\cos 2\psi$ pitch was applied. If substantiated in further tests, this behavior will also prove favorable to the use of $\cos 2\psi$ pitch for propulsive capability augmentation.

PRESENT AND FUTURE ROLE OF ANALYTICS

Until recently, it has been design practice to provide high torsional stiffness in rotor blades and to avoid bending-torsion couplings. These practices tended to minimize the effects of torsion upon load distributions. This in turn permitted the use of precalculated nonuniform downwash in the blade loads programs so far available to the designer. Prediction of the behavior of an aeroelastically activated rotor requires computation of the airloadings as affected by torsion. Thus the analytical design of such rotors requires computer programs with more sophistication than have been in common use.

The Boeing Vertol rotor loads program C-60 provides the essential coupling of torsion-to-flap bending and recalculates the bending airloads. It does not, however, iterate downwash as affected by the blade airload redistribution. Until modified in 1975 for the aeroelastically-adaptive rotor project, the program could not handle sweep of the outboard planform.

PREDICTION OF C_{M0} EFFECTS ON STRAIGHT BLADES

C-60 has been quite successful in predicting blade bending response to C_{M0} changes on the straight planform blades. Correlation with wind tunnel test data is shown in Figures 18 and 19. Figure 18 shows that, while the baseline alternating flap bending level is not well predicted, changes caused by ΔC_{M0} are predicted fairly accurately. Figure 19 shows that flap bending waveform prediction is also fairly accurate, with the notable exception of a segment on the advancing side. The consistent nature of the advancing blade waveform discrepancies in Figure 19 suggests the probability of a difference in baseline C_{M0} between the C-60 calculation and the actual model. Specifically, it appears that a negative shift of C_{M0} in both of the illustrated C-60 calculations would significantly improve the correlation.

Such a shift could be appropriate in view of the manner in which aerodynamic pitching moments were established for the C-60 calculation. The C-60 pitching moments apply to the airfoil section as designed, with an approximate adjustment for a small contour deviation known to be present in the mold used to fabricate the blades. The analytical moment adjustment should be refined as a part of future analytical work.

TRIMMED LEVEL FLIGHT AT $C_T/\sigma = 0.06$, $\bar{X} = 0.135$, HUB MOMENT = 0
2 BLADES, 1100 RPM

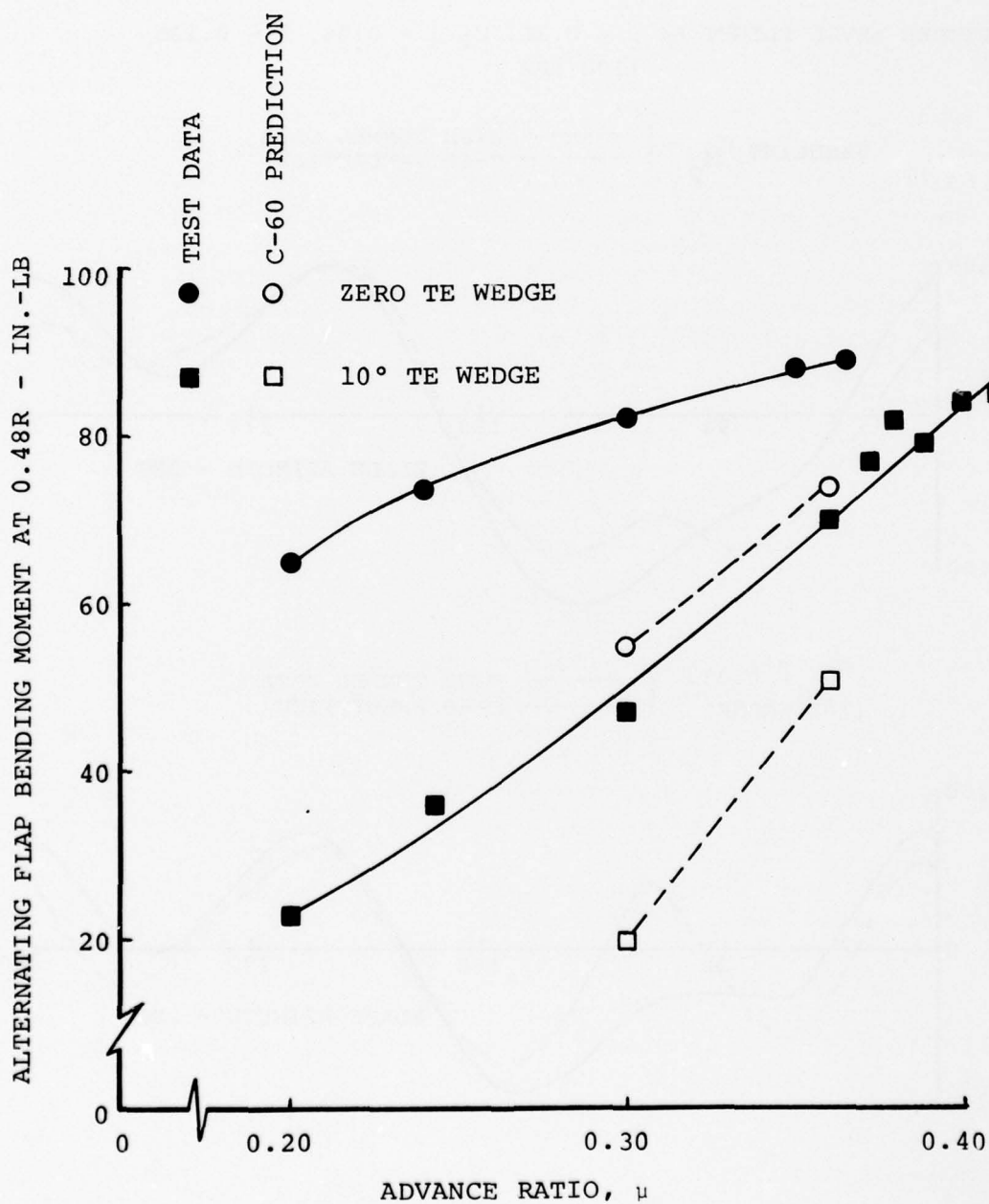
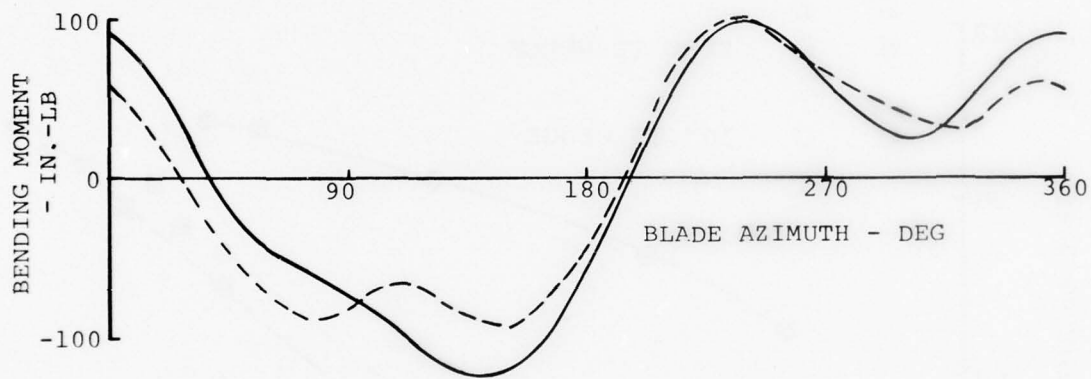


Figure 18. Alternating Flap Bending: C-60 Prediction Versus Wind Tunnel Data for Straight, Soft Blade (Design 6).

TRIMMED LEVEL FLIGHT AT $\mu = 0.36$, $C_T/\sigma = 0.06$, $\bar{X} = 0.135$
1100 RPM

BASELINE C_{M_0} { — WIND TUNNEL DATA
- - - C-60 PREDICTION



$\Delta C_{M_0} = 0.033$ (10° WEDGE) { — WIND TUNNEL DATA
- - - C-60 PREDICTION

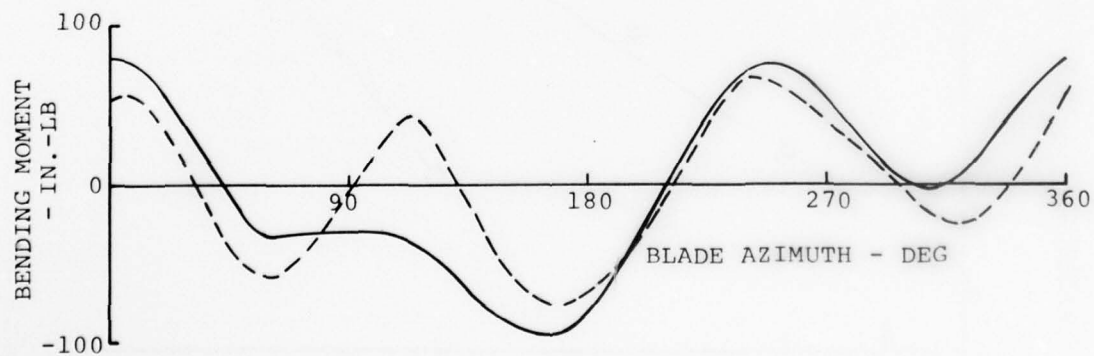


Figure 19. Flap Bending Waveform at 0.48R: C-60 Prediction Versus Wind Tunnel Data for Straight, Soft Blade (Design 6).

TORSION CALCULATION IS MOST ESSENTIAL

One product of the aeroelastically adaptive rotor wind tunnel test program is a clearer determination of the sophistication needed in programs such as C-60 to make them suitable analytical tools for the dynamics design of aeroelastically active rotors. Tentatively, it appears that downwash reiteration will not be as important as will the accurate calculation of blade torsional deflections. Thus it seems probable that when the sweep coupling of bending to torsion is accurately calculated, C-60 should predict overall swept-blade behavior with success comparable to the present straight-blade results. This expectation seems more firm for high advance ratio flight than for hover and transition where induced velocity effects should have larger interplay with the torsion due to sweep.

PREDICTION OF THE EFFECTS OF PLANFORM SWEEP

Of greater immediate importance is the need to predict the blade torsion and related effects which are introduced by sweep of the outboard planform. A C-60 planform sweep module was developed in 1975 and was applied to analyze the swept model blade tested under this program in 1976.

As tested, the swept blades displayed large three-per-rev torsional amplitudes at high rotor speed and when excited by retreating blade stall. This response in a lightly damped, coupled first torsion/second flap mode, with a natural frequency just above three-per-rev, was an adverse feature of the particular frequency map of these blades. The torsion was of a limit cycle nature, and loads were controlled by keeping rotor speed below that for three-per-rev resonance.

Correlation with C-60 analysis was impeded by the three-per-rev resonance problem. Like the model rotor, the C-60 calculation showed unusually large three-per-rev torsion and flap bending. However, the C-60 iterative process (which is designed to converge on a consistent set of airloads and blade motion) was less stable than the model rotor: the calculated three-per-rev deflections grew in amplitude exponentially from iteration to iteration, preventing convergence. The program could therefore not be used for direct correlation with measured loads. It could, however, be used to explore general characteristics of the resonance problem, since experience has shown that there is an approximate correspond-

ence between C-60 convergence behavior and actual physical stability.

C-60 convergence was found to be better at 750 rpm and 1432 rpm than at 1100 rpm, the rotor speed used for testing. Convergence was not satisfactory, however, even at the lower and higher rpm's, except in hover with the standard table lookup procedure for aerodynamic coefficients replaced by a simpler program option, linear aerodynamics with $C_M = 0$. Program options which have improved convergence in some cases in the past -- uniform downwash, structural damping, and bypass of the iterative rotor trim procedure -- yielded very little improvement. The rpm dependence of the convergence problem suggested that operation at rpm's above the resonance, as well as below the resonance, would be satisfactory. The results were quantitatively incorrect, however, in that test experience, unlike the program, showed that rotor stability was worse at 1432 rpm than at 1100 rpm.

The C-60 analysis was also used to determine sensitivity of the three-per-rev resonance problem to design changes. It was found that increasing blade torsional stiffness approximately five times to the UTTAS value greatly improved convergence, whereas increasing flap bending stiffness by as much as 10^4 was only moderately helpful. This indicated that the resonance was predominantly a torsional problem. Convergence was also greatly improved by removing outboard planform sweep from the program model (i.e., by changing from the Design 5 to the Design 6 configuration).

In light of the above, it appears that the C-60 program with the sweep module will probably be a useful tool for exploring the torsional and bending behavior of swept planform designs without instabilities. Confirmation of this will be sought during future tests of a stabilized, swept blade.

The stability of the swept blades was also investigated using programs Y-71 and Y-69. These are fully coupled blade analyses based on a lumped parameter model, with 25 spanwise blade sections. The programs solve the structural equations using a modified transfer matrix approach which includes a bend matrix between each pair of bays to represent finite deflections, such as sweep and twist, and a rigid offset matrix to represent variations of the center of mass, pitch axis, and elastic axis relative to each other. Y-71 omits the aerodynamics and determines in-vacuum mode shapes and natural

frequencies. Y-69 includes detailed perturbation aerodynamics for hover, with a table lookup procedure for aerodynamic coefficients, and determines modal damping as well as mode shapes and frequencies.

Y-69 calculations show a flap-torsion instability similar to that observed on the model, occurring at approximately the same rpm. The modal frequency map obtained from Y-69 is shown in Figure 20, which includes selected Y-71 results as a base-line in vacuum. The source of the Y-69 instability is aerodynamic coupling of the first flap and first torsion modes. At lower rpm's the coupling is such that torsion and flap are 180 degrees out of phase, producing a delta-three type effect. This effect increases with rpm, stiffening the first flap mode relative to the in-vacuum mode determined by Y-71 and raising the first flap frequency toward two-per-rev and finally beyond two-per-rev at about 1000 rpm. With further rpm increase, the relative phase between flap and torsion changes toward 90 degrees so the torsion begins to cause negative flap damping. The increasing negative damping finally causes instability at about 1350 rpm.

Unfortunately, some major aspects of the predicted instability are inconsistent with test experience and with C-60 results. The predicted instability occurs at 2.3-per-rev, whereas the observed instability was near 3-per-rev. Y-69 shows that removing sweep is destabilizing, whereas testing showed that it is stabilizing. Y-69 shows that the instability continues at high rpm, whereas C-60 indicates an improvement at high rpm. Finally, Y-69 shows that forward placement of the shear center is very destabilizing, whereas C-60 results are not sensitive to this parameter. For these reasons, it is concluded that there is a significant problem in the way the blade is currently modeled in the stability analysis. The modeling will be examined closely as the program continues, since it is believed that Y-71 and Y-69 are potentially very useful in dealing with the swept blade instability.

Results of a recent stability investigation of a flex-strap tail rotor design, incorporating blade sweep with the sweep apex near 0.25R, point to a significant physical effect which may not be properly modeled in the current analyses. It was found in the tail rotor investigation that the effective shear center of the strap was shifted significantly away from the strap centerline because the centrifugal force of the swept blade pulled on the strap at a skewed angle. Y-69 stability

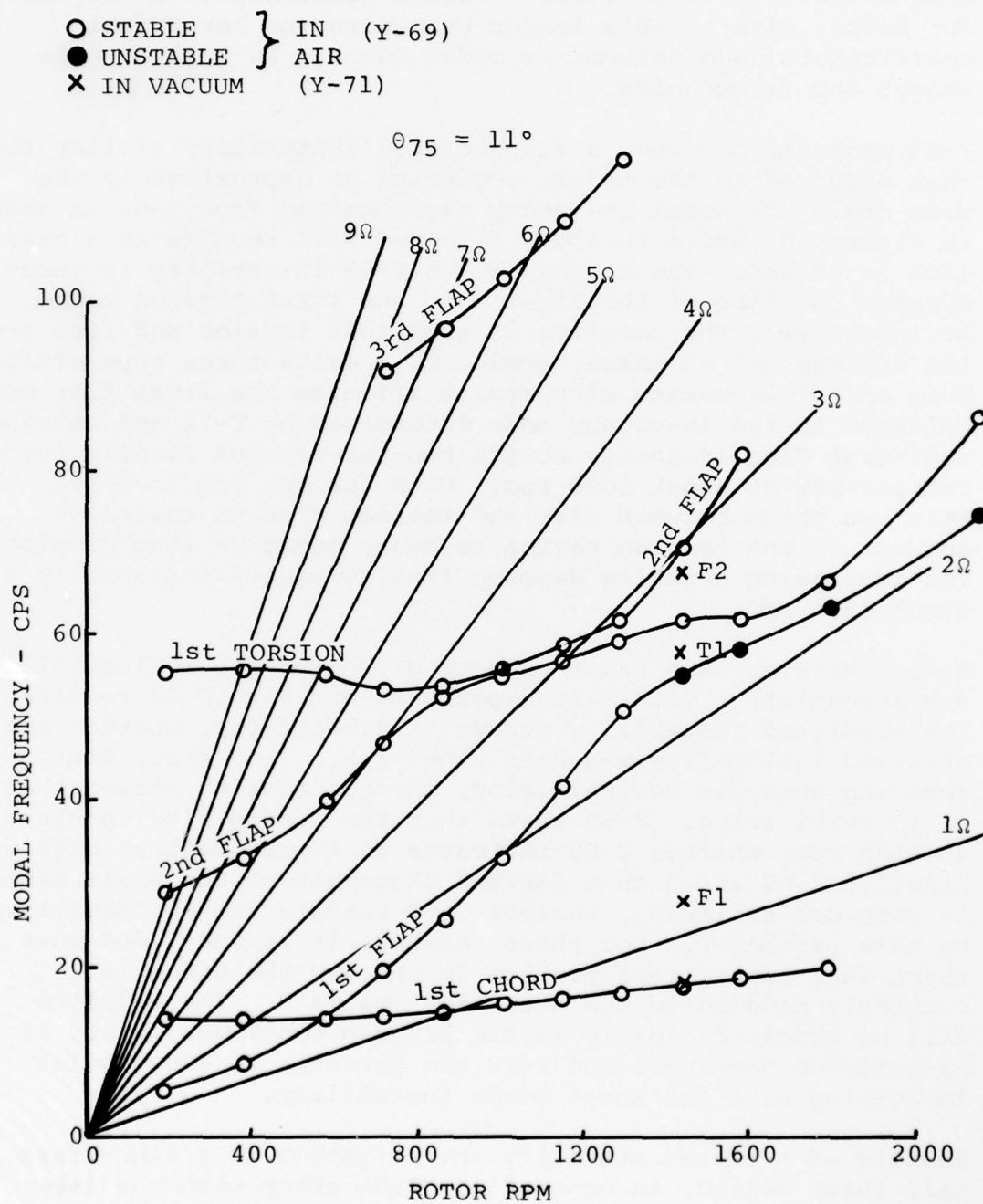


Figure 20. Modal Frequencies of Swept, Soft Blade (Design 5): Y69 and Y71 Predictions.

predictions, which had been inaccurate for the swept blade, were greatly improved when the shear center of the math model was moved away from the strap centerline. NASTRAN analysis was used to locate the shear center of the strap under the influence of a skewed centrifugal load. A similar shear center shift may be present in the swept tip blade tested for this program, although it has not been included in the analyses. This possibility will be investigated carefully in ongoing work.

GENERAL ADEQUACY OF ANALYTICAL TOOLS

For the present and near future aspects of aeroelastically adaptive rotor development, there is no important problem which arises from an inadequacy of analytical tools. There is a sufficiently clear understanding of the gross changes of rotor behavior which are needed. The blade design features which should induce the essential changes have been identified and demonstrated in the wind tunnel. They have also been explored by C-60 analysis with a degree of success which does not leave any critical engineering questions unanswered.

It is in the eventual refinement of an aeroelastically adaptive rotor design that more sophisticated, validated analytical programs will be helpful. For the present, the basic technology needed to apply the advantages of aeroelastic adaptivity can be obtained through parametric changes in wind tunnel models flown to their limits.

Full exploration of the limits in a wind tunnel program will serve to explore and illustrate the features that will be needed in future analytical programs.

ANALYTICAL STUDY OF DESIGN APPLICATIONS

IMPROVEMENT OF HOVER PERFORMANCE

The use of aeroelastically adaptive design to improve hover performance of straight blades has been explored using the C-60 program. The design approach, as noted earlier, has two elements:

- Static twist is increased for hover efficiency. This change increases flap bending loads in forward flight, principally by increasing tip down bending of the advancing blade.
- Noseup C_{M_0} is used to reduce flap bending loads to their original level, countering the effect of twist by reducing the tip down bending of the advancing blade. (The noseup C_{M_0} has an additional effect; it tends to reduce the steady twist, partially offsetting the hover performance gain achieved by the initial increase of static twist.)

Overall then, static twist is used to improve performance, C_{M_0} is used to reduce flap bending, and each of the changes (twist and C_{M_0}) has an adverse side effect which counteracts the primary desirable effect of the other. The relative sizes of the primary and side effects, and the net gain, predicted by C-60 for the straight soft blades as tested in the wind tunnel, are shown in Figures 21 and 22.

Figure 21 shows hover power requirement versus static twist and C_{M_0} . Note that if static twist is increased from 12 to 16 degrees with no change in C_{M_0} , hover power is reduced 4 percent. Figure 22, showing midspan flap bending moment at high speed versus static twist and C_{M_0} , shows that the same static twist change (from 12 to 16 degrees) increases flap bending by 14 percent. Figure 22 also shows, by interpolation, that $\Delta C_{M_0} = 0.0132$ lowers the flap bending of the 16-degree twist rotor to the level of the 12-degree twist rotor. The $\Delta C_{M_0} = 0.0132$, according to Figure 21, raises horsepower slightly to a level 3.1 percent below that of the 12-degree twist rotor. Thus, together the figures show that hover power can be reduced 3.1 percent without increasing midspan flap bending at high speed, by adding 4 degrees static twist, and $\Delta C_{M_0} = 0.0132$ (approximately 4 degrees upward tab deflection). This change does not, of course, represent a design optimization. It is rather an illustration of the effects which can be achieved. As another example, the following section describes an analytical study of the BO-105 helicopter, which predicted a

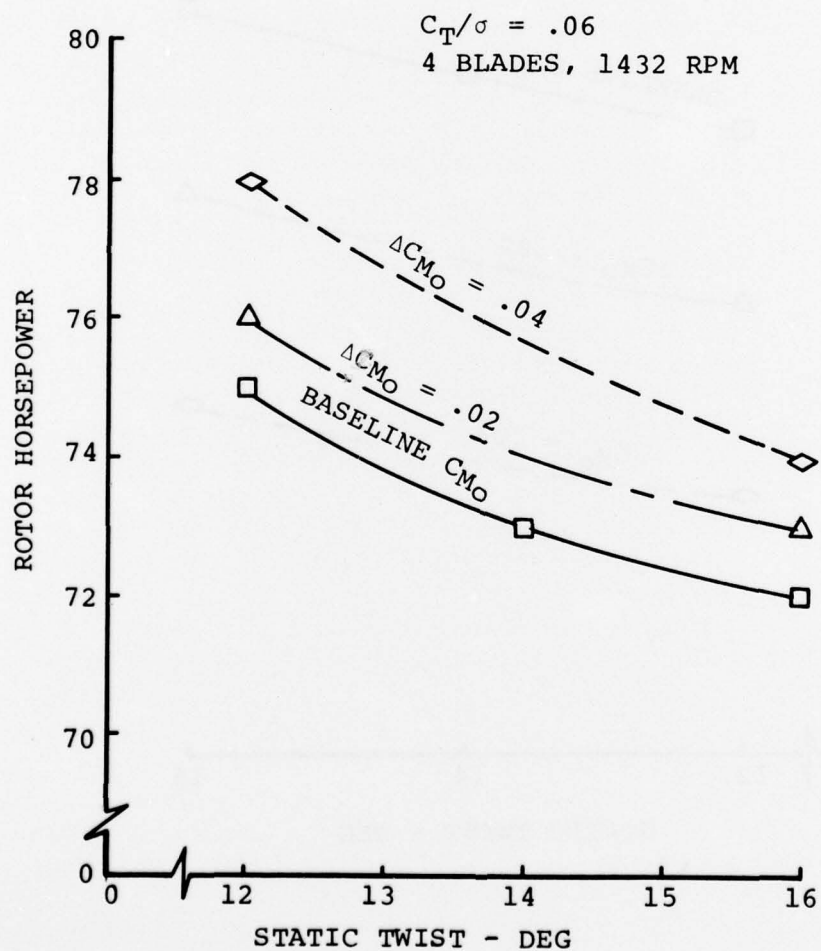


Figure 21. Hover Power Required Versus Static Twist and C_{M0} : C-60 Prediction for Straight, Soft Blade.

TRIMMED LEVEL FLIGHT AT $\mu = .36$, $C_T/\sigma = .06$, $\bar{X} = .1$,
HUB MOMENT = 0, 4 BLADES, 1432 RPM

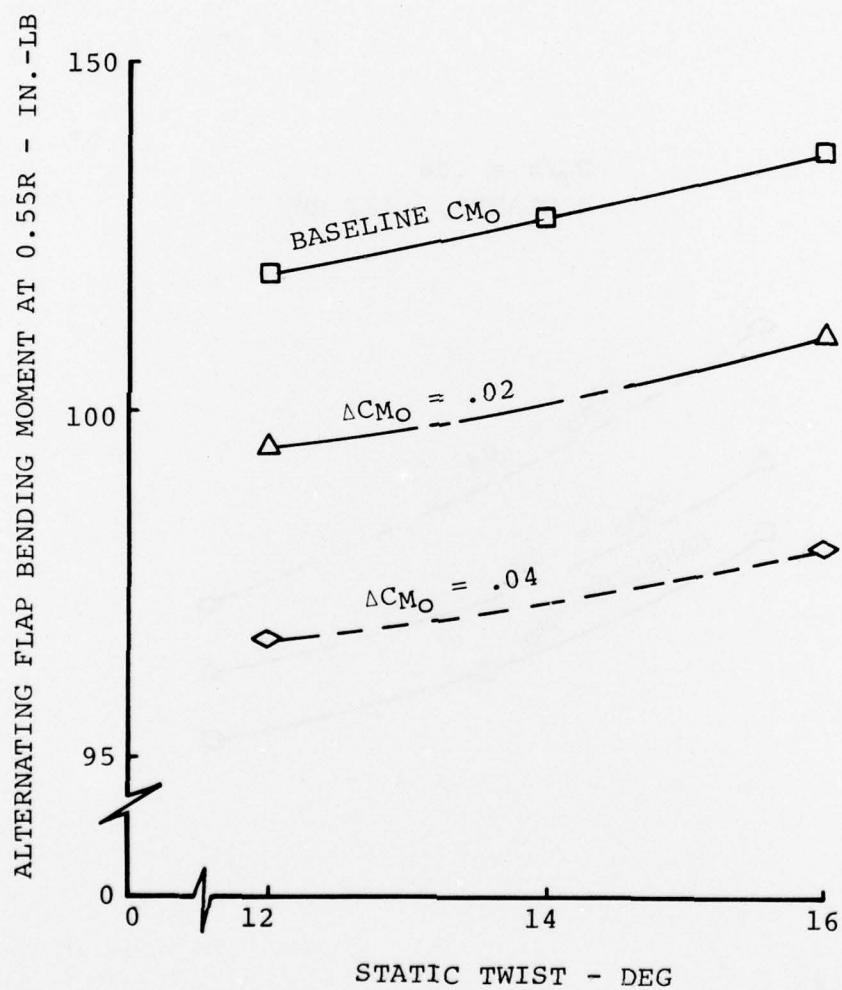


Figure 22. Alternating Midspan Flap Bending Versus Static Twist and CM_O : C-60 Prediction for Straight, Soft Blade.

hover power savings of about 6 percent due to increased twist.

REDUCTION OF FLAP BENDING AT HIGH SPEED

Noseup C_{M_0} and increased static twist can be combined in an alternate way to that just described. Forward flight flap bending can be reduced while maintaining the same hover performance rather than improving hover performance while maintaining the same flap bending. (More generally speaking, many C_{M_0} -twist combinations are possible, each of which achieves partial hover gains and partial flap bending gains in different proportions.)

For example, Figure 22 shows that adding $\Delta C_{M_0} = 0.04$ while maintaining 12-degree static twist reduces midspan flap bending moment at high speed by 43 percent. Figure 21, however, shows that this benefit is accompanied by a 4-percent increase in hover power required. It further shows through interpolation that hover power can be restored to its original value for baseline C_{M_0} by increasing blade static twist to 14.75 degrees. However, since increased static twist has an adverse effect on flap bending, improvement in the flap bending parameter is found to be reduced from 43 to 37 percent. In sum, increasing the static twist by 2.75 degrees while adding $\Delta C_{M_0} = 0.04$ (approximately 6-degree upward tab deflection) maintains hover performance while reducing midspan flap bending at high speed by 37 percent.

The above discussion calls attention to the fact that the measured flap bending reductions shown in Figures 5 and 8, which were achieved using tab deflections and trailing edge wedges on wind tunnel models, include a small reduction due to steady "untwist" of the blade by the C_{M_0} . (In the example above, the reduction due to steady effects was about 15 percent of the total reduction.) This part of the flap bending reduction would not, of course, be realized in practice because the designer would increase the built-in twist to achieve the same steady twist under load, thereby preserving hover efficiency.

COMBINED GAINS

As noted earlier, ΔC_{M_0} and increased static twist can be combined to achieve gains in hover performance and high-speed flap bending simultaneously. For example, Figures 21 and 22

together show that adding $\Delta C_{M_0} = 0.02$ while increasing static twist to 16 degrees has two beneficial results: hover power is reduced by 3 percent, and high-speed flap bending is reduced by 7 percent.

APPLICATION TO A DEMONSTRATION ROTOR

SELECTION OF A BASELINE HELICOPTER

The gains which can be obtained from application of aeroelastically adaptive principles are being examined by preliminary design analysis of a demonstration rotor. A study, still in process, has shown the impact upon design, performance, and productivity which could be expected from modification of a Boelkow/Boeing BO-105 helicopter.

The BO-105 is an appropriate baseline helicopter of advanced contemporary design. Its rotor system is the mature product of development and of service experience which has pushed it close to the practical limits. The tip speed of 716 fps results in moderate noise signature problems and penalizes hover performance. Advanced airfoil sections are used, but the static blade twist of only 8 degrees tends also to penalize hover performance. Essential data on the standard BO-105 and its rotor system are presented in Table 1.

TABLE 1. STANDARD BO-105 VEHICLE
AND ROTOR SYSTEM CHARACTERISTICS

Vehicle Characteristics

Normal gross wt, lb	5070
Weight empty, lb	2789
No. of engines/type	2 Allison Mod 250-C-20 T/shaft

Main Rotor Characteristics

Diameter, ft	32.2
No. of blades	4
Solidity/chord, in.	0.070/10.63
Twist, deg	-8
Airfoil	BV 23010-1.58

The fiberglass-composite rotor blade structure is very appropriate as a baseline design for aeroelastic improvement. The standard blade has a low torsional stiffness of approximately the level needed for aeroelastic adaptivity. Thus, there would be little change in the rotor blade structure and its response dynamics when modified.

The skid landing gear and utilitarian fuselage layout, with clamshell doors at the rear of the main fuselage, result in relatively high fuselage drag. The BO-105 is therefore a good choice for trial application where the desired gains are in hover performance, noise reduction, and maneuverability with reduced tip speed. Suitable tests of the rotor system where the goal is speed and range improvement would require major fuselage drag cleanup or the use of auxiliary propulsion to simulate drag reduction.

ADJUSTMENT OF TWIST AND TIP SPEED

The first attempt at design changes for performance improvement was directed to the adjustment of twist and tip speed. Blade planform and airfoil sections were left unchanged to get a view of what could be accomplished without disturbing the blade structure or basic blade response dynamics.

On the premise that flap bending in high-speed flight would be suppressed by C_{M_0} treatment, the rotor was optimized for hover efficiency at the normal 5070-pound gross weight. In a study utilizing the Boeing B-92 hover and SR1BR cruise performance analytical programs, it was found that the static linear twist should be increased to 18 degrees to optimize the induced power aspects of hover. Optimization of profile power was found to require a tip speed reduction to 600 fps.

The power required for hover decreased by 13 percent, with half the savings attributable to increased twist and the other half attributable to reduced tip speed. The power saved remained fairly constant out to 100 knots. Above that speed, the power required by the 600 fps rotor with torsionally rigid blades rose to match that of the 716 fps rotor at 135 knots. This deterioration of rotor efficiency reflects the SR1BR treatment of the earlier retreating blade stall and the increased twist of the higher advance ratio rotor. Because the program does not consider the improved load distribution due to dynamic twist, its prediction of level flight speed capability should be conservative.

PROPULSIVE CAPABILITY EFFECTS

The preceding discussion of the feasibility and attractiveness of the 600 fps, 18-degree twist rotor across the present level flight speed range of the BO-105 does not account for the likely reduction of the advance ratio levels and lift levels at which propulsive limits would be reached.

While it is unlikely that propulsive limits would inhibit level flight, it is expected that the maneuver envelope would be reduced at altitude. This effect will be probed in the next wind tunnel tests. If it proves to be a limit upon the otherwise flyable envelope it will be attacked by the introduction of second-harmonic pitch effects, to unload the retreating blade.

PROJECTED GAINS

Based solely upon the demonstrated effects of aeroelastic adaptivity, and discounting all prospective improvements of rotor aerodynamic efficiency in high-speed level flight, it is apparent that gains shown in Table 2 could be demonstrated in a BO-105 helicopter. Blades would be of present standard planform and airfoil section. Top-speed capability would be undiminished at 145 knots.

TABLE 2. GAINS ACHIEVABLE IN A BO-105 HELICOPTER USING AEROELASTICALLY ADAPTIVE DESIGN FEATURES

<u>At present normal gross wt, 5070 lb</u>	<u>Standard</u>	<u>Modified</u>	<u>% Gain</u>
Aural detection distance, ft*	7800	5200	33.3
Hover ceiling, ft	7900	9180	16.2
Vertical rate of climb, ft/min	410	1049	156.0
Maximum rate of climb, ft/min	1360	1603	17.9
Hover endurance, 800-lb payload, hr	3.50	3.96	13.3
Loiter time at 60 knots, 800-lb payload, hr	4.44	5.06	13.9

To produce original hover ceiling
(at 5309 lb gross weight)

Aural detection distance, ft*	7800	5200	33.3
Hover ceiling, ft	7900	7900	0
Vertical rate of climb, ft/min	410	677	65.0
Maximum rate of climb, ft/min	1360	1450	6.6
Hover endurance, 800-lb payload, hr	3.50	4.34	24.0
Loiter time at 60 knots, 800-lb payload, hr	4.44	5.50	23.9

NOTE: Performance at sea level standard where applicable.

- * 4db reduction is due to tip speed change alone, while ambient noise is assumed low enough to permit detection of the quiet rotor at 7200 feet.

CONCLUSIONS

Wind tunnel testing has shown that in a soft-inplane, hingeless rotor system, substantial improvements may be obtained from passive design features which create aeroelastic adaptivity to conditions encountered at high advance ratio.

STRAIGHT PLANFORM BLADES

For a wingless helicopter with blades of lowered torsional stiffness, with all propulsion provided by the rotor and with contemporary design conditions, $C_T/\sigma = 0.06$ and $\mu = 0.36$, testing has indicated that introducing a noseup aerodynamic pitching moment coefficient, C_{M_0} , of 0.033, has the following effects:

- Flap bending in the midspan area is reduced by
 - 43 percent at first harmonic
 - 40 percent at second harmonic
- The flying quality effects of the noseup C_{M_0} are generally favorable, consisting principally of an increase of vehicle speed stability.
- The accompanying redistribution of airloading across the rotor disc has only a small effect on the aerodynamic efficiency of the rotor at high advance ratio. But the reduction of flap bending loads can be sufficient to permit an increase of the design static twist to improve hover figure of merit.
- Simple theory indicates that the twist profiles which will create the above favorable effects would have an adverse effect upon the absolute propulsive limits of the rotor.

SWEPT PLANFORM BLADES

For the same design conditions, $C_T/\sigma = 0.06$ and $\mu = 0.36$, with C_{M_0} left at a nominally zero value, the testing has indicated that introducing a 10-degree sweep back of the outer 35 percent of the blade span has the following effects:

- Flap bending in the midspan area is reduced by
 - 10 percent at first harmonic
 - 30 percent at second harmonic

- Third-harmonic root flap bending in the second elastic mode is heavily attenuated both in transition from hover and at high advance ratio.
- Flying quality effects of the sweep are generally favorable, with speed stability increased and with conceivably favorable effects upon dynamic stability.
- Static twist increases with C_T , with potentially useful effects on performance.
- Static design twist can be increased to benefit aerodynamic performance, as a result of the reduction of flap bending loads.
- The phase of second-harmonic outboard flap bending in the subject testing was such that outboard sweep caused second-harmonic twist of a phase which did not unload the retreating blade. To use sweep for favorable effects on rotor limits, the spanwise mass distribution must be altered to shift the phase of second-harmonic flap bending.

COMBINATION OF SWEEP AND C_{M_0} EFFECTS

Of all configurations tested, the combination of outboard planform sweep and noseup C_{M_0} was found to achieve the lowest levels of outboard flap bending at first, second, and third harmonics. Planform sweep was also found to attenuate hub shaking loads in transition from hover to forward flight - an effect which was not significant with the C_{M_0} treatment alone. These effects of sweep are attractive and may contribute to an ultimate selection of sweep in combination with C_{M_0} and other aeroelastic activity sources.

RETENTION OF PROPULSIVE CAPABILITY

Further investigation is required to quantify the effects upon propulsive capability when twist is introduced for bending suppression or L/D_E improvement. This aspect of the introduction of dynamic twist was beyond the scope of the initial testing and will require a model mechanically capable of flying to the limits. Evaluation of the full effects upon helicopter productivity will involve the following:

- The advance ratio margins actually available for productivity improvement and noise reduction will

depend upon any adverse change in the propulsive limits.

- Confirmation of the value of second-harmonic blade root pitch control as a means of opening the propulsive limits must be quantified during anticipated testing of the effects of dynamic twist upon those limits.

COMPATIBILITY OF SECOND-HARMONIC ROOT PITCH CONTROL

Testing to date indicates that second-harmonic pitch control has the anticipated qualitative effects on trim when applied below the propulsive limits. Its functioning appears to be compatible with the torsionally soft, unswept blades but it has not yet been tested on the swept blades.

LIST OF SYMBOLS

A_1	lateral cyclic pitch, deg
B_1	longitudinal cyclic pitch, deg
C_T	rotor thrust coefficient
C_{M_0}	aerodynamic pitching-moment coefficient at zero thrust
D_E	rotor equivalent drag, lb
L	rotor lift, lb
R	rotor radius, ft
X	rotor propulsive force, lb
\bar{X}	rotor propulsive-force coefficient, $X/qd^2\sigma$
$\theta_{.75}$	collective pitch at $0.75R$, deg
μ	ratio of forward speed to tip speed
σ	rotor solidity
ψ	blade azimuth angle leaving tail, deg
Ω	main rotor speed, rad/sec
ω_t	first-mode torsional blade frequency, rad/sec